



1 **The EMEP Intensive Measurement Period campaign,**
2 **2008–2009: Characterizing the carbonaceous aerosol at**
3 **nine rural sites in Europe**

4 Karl Espen Yttri^{*a}, David Simpson^{b,c}, Robert Bergström^{c,d}, Gyula Kiss^e, Sönke
5 Szidat^f, Darius Ceburnis^g, Sabine Eckhardt^a, Christoph Hueglin^h, Jacob Klenø
6 Nøjgaardⁱ, Cinzia Perrino^j, Ignazio Pizzo^a, Andre Stephan Henry Prevot^k, Jean-
7 Philippe Putaud^l, Gerald Spindler^m, Milan Vanaⁿ, Yan-Lin Zhang^{jk}, Wenche Aas^a

8

9 ^aNILU — Norwegian Institute for Air Research (NILU), N-2027 Kjeller, Norway

10 ^bNorwegian Meteorological Institute, 0313 Oslo, Norway

11 ^cDepartment of Space, Earth and Environment, Chalmers University of Technology, 41296 Gothenburg

12 ^dSwedish Meteorological and Hydrological Institute, 60176 Norrköping, Sweden

13 ^eMTA-PE Air Chemistry Research Group, 8200 Veszprém – Hungary

14 ^fDepartment of Chemistry and Biochemistry & Oeschger Centre for Climate Change Research,
15 University of Bern, 3012 Berne, Switzerland

16 ^gSchool of Physics and Centre for Climate and Air Pollution Studies, Ryan Institute, National
17 University of Ireland Galway, Galway, Ireland

18 ^hEMPA, CH-8600 Dübendorf, Switzerland

19 ⁱNational Environmental Research Institute, DK-4000 Roskilde, Denmark

20 ^jCNR — Institute of Atmospheric Pollution Research, 00015 Monterotondo Stazione (Rome), Italy

21 ^kPaul Scherrer Institut, 5232 Villigen-PSI, Switzerland

22 ^lEuropean Commission, Joint Research Centre, I-21027 Ispra (VA), Italy

23 ^mLeibniz Institute for Tropospheric Research, 04318 Leipzig, Germany

24 ⁿThe Czech Hydrometeorological Institute (CHMI), Prague, Czech Republic

25

26 ^{*}To whom correspondence should be addressed: E-mail address: key@nilu.no

27

28 **Abstract**

29 Source apportionment (SA) of carbonaceous aerosol was performed as part of the EMEP Intensive
30 Measurement Periods (EIMPs), conducted in fall 2008 and winter/spring 2009. Levels of elemental
31 carbon (EC), particulate organic carbon (OC_p), particulate total carbon (TC_p), levoglucosan and ¹⁴C in
32 PM₁₀, observed at nine European rural background sites, were used as input for the SA, whereas Latin
33 Hypercube Sampling (LHS) was used to statistically treat the multitude of possible combinations
34 resulting when ambient concentrations were combined with appropriate emission ratios. Five
35 predefined sources/subcategories of carbonaceous aerosol were apportioned: Elemental and organic
36 carbon from combustion of biomass (EC_{bb} and OC_{bb}) and from fossil fuel (EC_{ff} and OC_{ff}) sources, as
37 well as remaining non-fossil organic carbon (OC_{mf}), typically dominated by natural sources.

38 The carbonaceous aerosol concentration decreased from South to North, as did the concentration
39 of the apportioned carbonaceous aerosol. OC_{mf} was more abundant in fall compared to winter/spring,
40 reflecting the vegetative season, and made a larger contribution to TC_p than anthropogenic sources
41 (here: EC_{bb}, OC_{bb}, EC_{ff} and OC_{ff}) at four of the sites, whereas anthropogenic sources dominated at all
42 but one sites in winter/spring. Levels of OC_{bb} and EC_{bb} were typically higher in winter/spring than in
43 fall, due to larger residential wood burning emissions in the heating season, whereas there was no
44 consistent seasonal pattern for fossil fuel emissions. Biomass burning (OC_{bb} + EC_{bb}) was the major
45 anthropogenic source at the Central European sites in fall, whereas fossil fuel sources dominated at the
46 southernmost and the two northernmost sites. In winter/spring, biomass burning was the major
47 anthropogenic source at all but two sites. Addressing EC in particular, fossil fuel sources dominated at
48 all sites in fall, whereas there was a shift towards biomass burning in winter/spring for the
49 southernmost sites. Influence of residential wood burning emissions was substantial already in the first
50 week of sampling in fall, constituting 30 – 50% of TC_p at most sites, showing that this source can be
51 dominating even at a time of the year when the ambient temperature in Europe is still rather high.

52 Model calculations were made, attempting to reproduce LHS-derived OC_{bb} and EC_{bb}, using two
53 different residential wood burning emission inventories. Both simulations strongly under-predicted the
54 LHS-derived values at most sites outside Scandinavia. Emissions based on a consistent bottom-up
55 inventory for residential combustion (and including intermediate volatility compounds, IVOC)
56 improved model results at most sites compared to the base-case emissions (based mainly on officially
57 reported national emissions), but at the three southernmost sites the modelled OC_{bb} and EC_{bb}
58 concentrations were still much lower than the LHS source apportioned results.

59 The current study shows that natural sources is a major contributor to the carbonaceous aerosol in
60 Europe even in fall and in winter/spring, and that residential wood burning emissions can be equally
61 large or larger than that of fossil fuel sources, depending on season and region. Our results suggest that
62 residential wood burning emissions are still poorly constrained for large parts of Europe. The need to
63 improve emission inventories is obvious, with harmonization of emission factors between countries
64 likely being the most important step to improve model calculations, not only for biomass burning
65 emissions, but for European PM_{2.5} concentrations in general.

66



67 **Introduction**

68 Atmospheric aerosol particles play an important role in a number of environmental topics such as the
69 radiation transfer of the Earth's atmosphere, the hydrological cycle as well as air quality, and thus have
70 a substantial impact on the biosphere, including human health (Pope and Dockery, 2006; Andreae and
71 Ramanathan, 2013). Carbonaceous matter is an important component of aerosol particles that has been
72 found to account for 10–40% of PM₁₀ in the European rural background environment, 20–50% of
73 PM_{2.5} in urban and rural locations, and up to 70% of PM₁ (Zappoli et al., 1999; Putaud et al., 2010;
74 Yttri et al., 2007a; Zhang et al., 2007; Querol et al., 2009). The carbonaceous matter is the least
75 understood fraction of atmospheric aerosol particles due to its complexity in terms of composition,
76 sources and formation mechanisms (Gelencsér, 2004; Pöschl, 2005; Hallquist et al., 2009; Ziemann
77 2012). Nevertheless, it is considered to have specific impacts on global climate (Novakov and Penner,
78 1993; Kanakidou et al., 2005), and on human health (Bell et al., 2009; Rohr and Wyzga, 2012; Cassee
79 et al., 2013).

80 Particulate carbonaceous matter covers a wide range of organic components from low molecular
81 weight hydrocarbons, through complex mixtures of humic-like substances and high molecular weight
82 biopolymers containing also oxygen, nitrogen and sulphur, to tar balls or particles consisting of
83 graphene layers. This continuum in chemical composition is reflected also in its thermochemical and
84 optical properties (Pöschl et al., 2003). The carbonaceous fraction is usually quantified by its carbon
85 content (total carbon, TC), which can be operationally divided into carbonate, organic carbon (OC),
86 and elemental (EC) or black carbon (BC).

87 The complexity of carbonaceous aerosol originates from the diversity of its sources and formation
88 processes. Carbonaceous particles are emitted both from anthropogenic (e.g. fossil fuel and biomass
89 combustion) and biogenic sources (e.g. primary biological aerosol particles, PBAP, such as fungal
90 spores, bacteria and degraded plant material). In addition to primary aerosol (emitted in particle form),
91 carbonaceous aerosol can form by atmospheric oxidation of volatile precursors emitted by the
92 vegetation or anthropogenic sources. Because of its climate forcing and adverse health effects, as well
93 as its considerable contribution to particulate mass, source apportionment of carbonaceous aerosol is of
94 key importance. By ¹⁴C-analysis, carbonaceous aerosol from fossil and modern sources can be
95 distinguished and quantified (Szidat et al., 2004; Szidat et al., 2009; Heal et al., 2011), and whereas
96 fossil carbon is only emitted as a consequence of human activities, modern carbon originates from both
97 biogenic and anthropogenic sources. Thus, source-specific tracers are necessary to apportion the
98 modern carbon content. Levoglucosan, characteristic for wood burning emission, is the most
99 commonly used macrotracer, whereas arabinol, mannitol and cellulose are used to distinguish different
100 types of PBAP, another source of contemporary carbon. The combination of ¹⁴C and source-specific
101 organic tracer analysis has proved to be an efficient method for source apportionment of the
102 carbonaceous aerosol (Gelencsér et al., 2006; Gilardoni et al., 2011; Yttri et al. 2011a, b; Liu et al.,
103 2016). Studies combining ¹⁴C- and ¹³C-analysis for source apportionment are also reported (Ceburnis et
104 al. 2011).

105 Globally, biomass burning is the major source of the carbonaceous aerosol (Crutzen and Andreae,
106 1990; Gelencsér, 2004), but the form and volume combusted (savanna fires, tropical forest fires,



107 agricultural waste burning, residential wood burning, etc.) depend highly on the geographical position,
108 climate and economic situation. In Europe, wood burning for residential heating, wild fires and
109 agricultural waste burning are the dominant forms of biomass burning, and thus significant sources of
110 carbonaceous aerosol, although these sources were hardly recognized for large parts of Europe, until
111 recently. Reviewing source apportionment studies of particulate matter in Europe between 1987 and
112 2007, Viana et al. (2008) stated that in spite of its importance at certain locations, biomass combustion
113 had rarely been identified as a substantial contributor to PM levels. Gelencsér et al. (2007) and May et
114 al. (2009) studied anthropogenic versus natural contribution to the total organic carbon content in
115 aerosol samples collected at six non-urban sites along a west-east transect over Europe from the Azores
116 (Portugal) to K-puszta (Hungary) and found biogenic sources to dominate at all sites in summer. In
117 winter most of the carbonaceous aerosol was emitted from anthropogenic sources, but there was a
118 considerable difference in the contribution of biomass burning and fossil fuel combustion, depending
119 on the geographical location (primarily altitude) of the sampling sites. Recently, a number of
120 measurement based studies have discussed the role of residential wood burning as a source of air
121 pollution in European urban and rural environments. As an example, road traffic and wood combustion
122 contributed equally to the annual mean PM₁₀ concentrations at various sites in Switzerland (Gianini
123 et al., 2012). In rural environment in the Alps, the contribution of wood burning to PM₁₀ even exceeded
124 that of road traffic (Gianini et al., 2012), and in Alpine valleys wood burning was the dominant source
125 of carbonaceous particles in wintertime (Szidat et al., 2007; Gilardoni et al., 2011; Herich et al., 2014;
126 Zotter et al., 2014). Similar results were found both in rural and urban environments in Norway by Yttri
127 et al. (2011a), who concluded that 80–90% of the winter time carbonaceous aerosol was emitted from
128 anthropogenic sources, and that wood burning contributed slightly more than fossil-fuel sources. In
129 summer, however, 70% of TC was attributed to natural sources in the rural environment, whereas the
130 corresponding number for the urban environment was 50%.

131 Modelling studies from recent years confirm that wood burning emissions are important in
132 wintertime Europe, and that such emissions seem to be severely underestimated in many regions
133 (Simpson et al., 2007; Bergström et al., 2012; Genberg et al., 2013). Denier van der Gon et al. (2015a)
134 pointed at inconsistent emission factors as a major problem (some countries report mainly solid
135 emissions, whereas others include substantial amounts of condensed semi-volatile OC, SVOC), and
136 produced a new bottom-up emission inventory for residential wood burning emissions of OC and EC,
137 using a consistent methodology across Europe (see also Genberg et al., 2013). Modelling work based
138 upon this inventory, and also including associated intermediate volatility compounds (IVOC),
139 improved model results for both EC and OC at European regional background sites (Genberg et al.,
140 2013 and Denier van der Gon et al., 2015a) but, so far, only limited comparisons to source
141 apportionment data have been made with model simulations using the new inventory.

142 The EMEP (European Measurement and Evaluation Program) task force on measurement and
143 modelling (TFMM) periodically arranges intensive measurement periods (IMPs), as a supplement to
144 the continuous monitoring in EMEP (Aas et al., 2012). The present study is part of the second EMEP
145 IMP, which was organized in cooperation with the EU-funded project EUCAARI (European Integrated
146 project on Aerosol, Cloud, Climate, and Air Quality Interactions: Kulmala et al., 2009; Crippa et al.,



147 2014) in fall 2008 and winter/spring 2009. In this study, collection of aerosol filter samples and
148 measurements of ^{14}C , levoglucosan and OC/EC were harmonized by common protocol and analysis in
149 centralized laboratories. The objective was to provide quantitative estimates of carbonaceous aerosol
150 from fossil fuel, biomass burning and natural sources in the European rural background environment,
151 and to study their relative contribution in two transition periods, in which a noticeable signal from all
152 the considered sources was expected. The carbonaceous aerosol apportioned to biomass burning was
153 used to evaluate model simulated EC_{bb} and OC_{bb} with both a base-case emission inventory, based
154 mainly on official nationally reported emissions, and a recent, consistent, bottom-up estimate of
155 residential combustion emissions. In the current paper we present the main findings from our study.

156

157 1. Experimental

158 1.1 Site description and measurement period

159 Aerosol filter samples were collected at nine European rural background sites (Table 1, Figure 1) for a
160 fall period (17 September–15 October 2008; denoted Fall) and a winter/spring period (25 February–25
161 March 2009; denoted Winter/spring). For a description of the sampling sites, see Appendix A.

162

163 1.2 Aerosol sampling

164 Ambient aerosol filter samples were obtained using various low volume filter samplers equipped with a
165 PM_{10} inlet, collecting aerosol on pre-fired (850 °C; 3 h) quartz fiber filters (Whatman QMA; 47 mm in
166 diameter, batch number 11415138). The only exception was for samples collected at the Mace Head
167 station, which used a high volume sampler with a $\text{PM}_{2.5}$ inlet. The samplers were operated at a flow
168 rate ranging from 16.7 l min^{-1} to 1.71 m³ min^{-1} , corresponding to a filter face velocity ranging from 20
169 to 69 cm s^{-1} (Table 1). The filter samples were collected according to the Quartz fiber filter behind
170 Quartz fiber filter (QBQ) approach to provide a quantitative estimate of the positive sampling artefact
171 of organic carbon (OC), thus the impact of the different filter face velocities at the various sites should
172 be minimized. The sampling time was one week, and four samples were collected at each site for each
173 of the two periods. At Mace Head, the collection of filter samples deviated slightly from the protocol in
174 Fall 2008, as the second week of sampling was divided into two to separate polluted air masses passing
175 over the European continent for the first three days of the week and clean marine air masses for the last
176 four days of the week. The sampling inlets were installed approximately 4 m above ground level,
177 except at Mace Head (10 m). Post exposure, filter samples were placed in petri-slides and stored in a
178 freezer (-18 °C) to prevent degradation or evaporation of the analytes.

179

180 1.3 Thermal-optical analysis

181 Total carbon (TC), elemental carbon (EC), and organic carbon (OC) were quantified using the Sunset
182 Lab OC-EC Aerosol Analyzer (Birch and Cary, 1996), using transmission for charring correction and
183 operated according to the EUSAAR-2 temperature program (Cavalli et al., 2010)

184



185 1.4 Determination of non-fossil TC from ^{14}C analysis

186 For the measurement of $^{14}\text{C}(\text{TC}_p)$ (^{14}C of particulate TC), 0.2–2 cm² punches, corresponding to 4–40
187 µg TC, were transferred into preheated quartz tubes (4 mm outer diameter) filled with ~0.1 g cupric
188 oxide. The tubes were connected to a vacuum line, cooled to -70 °C, evacuated to <10⁻³ hPa within one
189 minute and then sealed. The sealed ampoules were heated to 850 °C for 4 hours for oxidation of TC to
190 carbon dioxide (Fahrni et al., 2010). ^{14}C measurements were performed at the Laboratory of Ion Beam
191 Physics of ETH Zurich, using the accelerator mass spectrometer MICADAS, equipped with a gas ion
192 source (Ruff et al., 2007), which allowed a direct injection of the carbon dioxide after dilution with
193 helium (Wacker et al., 2013). ^{14}C results for the front filters were corrected for SVOC contributions
194 using the TC mass of the corresponding back filters and the mean ^{14}C result of the four back filters for
195 the respective site and season. $^{14}\text{C}(\text{TC}_p)$ values are given as fractions modern ($F^{14}\text{C}$), i.e. as the $^{14}\text{C}/^{12}\text{C}$
196 ratios of the samples related to the isotopic ratio of the reference year 1950 (Reimer et al., 2004). For
197 determination of the non-fossil fraction of TC_p (i.e., $f_{\text{nf}}(\text{TC}_p)$ from $^{14}\text{C}(\text{TC}_p)$ determinations, a reference
198 $F^{14}\text{C}$ value of pure non-fossil emissions of 1.08 ± 0.04 was used to consider the different impacts of
199 excess ^{14}C from atmospheric nuclear bomb tests to fresh biomass and tree wood (Mohn et al., 2008).
200 This is based on the assumptions that 50% of non-fossil TC originates from fresh biomass and 50%
201 from burning of wood, whereof the latter includes 10-year, 20-year, 40-year, 70-year and 85-year old
202 trees with weights of 0.2, 0.2, 0.4, 0.1, and 0.1, respectively.

203

204 1.5 Measurement of levoglucosan, mannosan and galactosan

205 Quantification of the monosaccharide anhydrides (MA) levoglucosan, mannosan and galactosan was
206 performed according to the method described by Dye and Yttri (2005), which has been successfully
207 applied for aerosol samples ranging from the urban (e.g. Fuller et al., 2014) to the remote environment
208 (e.g. Yttri et al. 2014).

209 For the analysis, punches (1.5 cm²) of the filter were spiked with $^{13}\text{C}_6$ -levoglucosan and $^{13}\text{C}_6$ -
210 galactosan and extracted twice with 2 ml tetrahydrofuran under ultrasonic agitation (30 min). The
211 filtered extracts (Teflon syringe filter, 0.45 µm) were evaporated to a total volume of 1 ml in a nitrogen
212 atmosphere. Before analysis the sample solvent elution strength was adapted to the mobile phase by
213 adding Milli-Q water (0.8 ml). The concentrations of the MAs were determined using High-
214 Performance Liquid Chromatography (HPLC) (Agilent model 1100) in combination with HRMS-TOF
215 (high resolution time-of-flight mass spectrometry, Micromass model LCT) operated in the negative ESI
216 mode. Levoglucosan, mannosan and galactosan were identified on the basis of retention time and mass
217 spectra of authentic standards. Quantification was performed using isotope labeled standards of
218 levoglucosan and galactosan. The mass traces at m/z 161.0455 and 167.0657 were used for
219 quantification (approximately 50 mDa peak width).

220 The method described has been subject to intercomparison (Yttri et al., 2015).

221



222 **1.6.1 Measurement uncertainties**

223 **1.6.1 Estimating the positive sampling artefact of OC**

224 Table 2a and b show the OC_{Back}/OC_{Front} ratios for the various sites. OC_{Back} is gaseous OC present on the
225 back filter and OC_{Front} is the sum of gaseous and particulate OC on the front filter. This ratio provides
226 an estimate of the magnitude of the positive sampling artefact (i.e. adsorption of semi volatile organic
227 species on the filter/ collected particles) of OC when using tandem filter sampling. When subtracting
228 OC_{Back} from OC_{Front} , positive-artefact-corrected particulate organic carbon (OC_p) is obtained.

229 The positive artefact of OC ranged from 5.9 ± 1.0 % (K-puszt, HU) to 28 ± 13 % (Lille Valby,
230 DK) in fall, whereas the corresponding range in winter/spring was 6.6 ± 1.3 % (Ispra, IT) to 30 ± 10 %
231 (Lille Valby, DK). This shows that OC_p could be severely overestimated if the positive artefact was not
232 accounted for. Note that the QBQ approach does not account for any negative artefacts (i.e. release of
233 semi volatile organic species from collected particles), thus the OC_p levels should be considered as
234 conservative estimates. There was typically a minor difference in the magnitude of the positive artefact
235 between fall and winter/spring. No seasonal pattern consistent for all sites was observed.

236

237 **1.6.2 Uncertainties in OC/EC measurements**

238 $\sim 15 \mu\text{g EC cm}^{-2}$ is considered the upper limit for the Sunset Lab OC-EC Aerosol Analyzer
239 (Subramanian et al., 2006; Wallén et al., 2010), and should not be exceeded in order to obtain a correct
240 OC/EC split. A non-biased OC/EC split also requires that either pyrolytic carbon (PC) evolves before
241 EC or that PC and EC have the same light absorption coefficient, which we know is not always the case
242 (Yang and Yu, 2002). In Fall 2008 11/36 samples exceeded $15 \mu\text{g EC cm}^{-2}$, whereas the corresponding
243 number for winter/spring 2009 was 3/36. For most of these samples the concentration just barely
244 exceeded $15 \mu\text{g EC cm}^{-2}$, nevertheless there is an added, non-quantifiable, uncertainty for these
245 samples compared to those for which $EC < 15 \mu\text{g C cm}^{-2}$.

246

247 **1.6.3 Uncertainties in levoglucosan analysis**

248 Yttri et al. (2015) reported that the analytical method used to quantify levoglucosan in the current study
249 had a bias of $-13\pm 4\%$ compared to the assigned value, being the median value of levoglucosan based on
250 the values reported by all participating laboratories in the actual intercomparison.

251

252 **1.6.4 Uncertainties of the $f_{nf}(TC_p)$ determination from ^{14}C analysis**

253 Uncertainties of $^{14}\text{C}(TC)$ measurements were 1–4% for the front filters and 2–10% for the pooled back
254 filters. The uncertainties of the front filters increased upon calculation of $^{14}\text{C}(TC_p)$, especially for filters
255 with high SVOC contributions. A further increase occurred when determining $f_{nf}(TC_p)$ (f_{nf} = fraction
256 non fossil) due to the uncertainty of the reference f_M value of pure non-fossil emissions so that the final
257 uncertainties of the non-fossil fraction of TC_p given in Table 2a and b ranged from 0.03 to 0.09.

258 Two samples from Birkenes and two from Košetice had unrealistically high ^{14}C values, for
259 unknown reasons. This finding was confirmed when rerunning the samples at another research
260 institute. There are other examples showing that super modern carbon can be an issue for TC measured
261 at European rural background sites (e.g. Glasius et al., 2018). Several hypothesis were suggested with



262 respect to what are the sources of super-modern carbon in the atmosphere: e.g. emissions from nuclear
263 power plants, waste incinerators taking care of waste from laboratories and hospitals, and crematoriums
264 (Buchholz et al., 2013; Zotter et al., 2014). Although samples highly contaminated with super-modern
265 ^{14}C are easily observed, it is not possible to determine if reasonable looking samples are free from such
266 contamination. ^{14}C contaminated measurements may lead to an overestimation of sources that emit
267 modern carbon when performing source apportionment of the carbonaceous aerosol, as described in the
268 current paper.

269

270 **1.7 Chemical transport modelling**

271 An important use of the carbonaceous aerosol Latin Hypercube Sampling (LHS) based source
272 apportionment, is to evaluate and constrain model systems for simulating particulate matter in the
273 atmosphere. The EMEP MSC-W model (Simpson et al., 2012; 2017 and references therein) is an Open
274 Source chemical transport model widely used for research, within the EMEP programme, and
275 elsewhere (e.g. Simpson et al., 2007; Bergström et al., 2012; 2014; Dore et al., 2015; Ots et al., 2016;
276 Vieno et al., 2016). In the present study we run the EMEP model with a horizontal resolution of 50 km
277 \times 50 km across Europe, using 21 vertical levels, the lowest level being approximately 50 m thick.
278 Meteorological data from the Integrated Forecast System model (IFS; Cycle 40r1) of the European
279 Centre for Medium-Range Weather Forecasts (ECMWF) were used to drive the model. For this study,
280 version rv4.15 of the model was used with some modifications: The OC emissions from all sources
281 (except wildfires and open agricultural fires, which were treated as non-volatile for simplicity) were
282 treated as semi-volatile, and subject to evaporation and oxidation in the gas-phase (ageing), using a
283 volatility basis set (VBS) approach, similar to the VBS PAA scheme in Bergström et al. (2012; the
284 PAA scheme includes gas-particle Partitioning of primary organic aerosol emissions and Aging of All
285 semi-volatile OA components in the gas-phase). The model was run for the years 2008 and 2009, with
286 two different emission set-ups (See Sects. 2.7.1.1 and 2.7.1.2) in order to evaluate model performance
287 for biomass-burning derived OC and EC with these inventories.

288

289 **1.7.1 Emissions**

290 European residential wood burning inventories have substantial inconsistencies between countries
291 (Denier van der Gon, 2015a; Simpson and Denier van der Gon, 2015), and several assumptions
292 concerning volatility and oxidation-processes for such emissions are possible (e.g. Robinson et al.,
293 2007; Grieshop et al., 2009; Bergström et al., 2012; May et al. 2013a; Jathar et al., 2014; Ciarelli et al.,
294 2017). To illustrate some of the uncertainties associated with this, two different emission set-ups were
295 applied in the present study: A base-case run using the widely used MACC-III emission inventory, and
296 an alternative run, denoted DT+IVOC.

297 In both cases, anthropogenic emissions (except as noted below) were based on the TNO
298 MACC emission inventory for 2011 (Kuenen et al., 2014; Denier van der Gon et al., 2015b) with
299 emission categories following the SNAP system, in which SNAP-2 includes non-industrial combustion,
300 such as residential wood burning. Emissions from vegetation fires and agricultural burning were taken



301 from the Fire INventory from NCAR version 1.5 (FINNV1.5; Wiedinmyer et al., 2014) and OC
302 emissions from these types of fires were treated as non-volatile.

303

304 1.7.1.1 Base Case

305 For SNAP-2, the MACC-III emissions were split into biomass burning sources (mainly wood and
306 woody fuels) and fossil fuel sources (coal, oil etc.), using data from Kuenen (pers. comm., 2017). The
307 emissions in MACC-III were split into five volatility bins, with saturation concentrations (C_{298K}^* , in the
308 range 0.01–1000 $\mu\text{g m}^{-3}$) as shown in Table 3.

309

310 1.7.1.2 DT+IVOC Case

311 POA and EC SNAP-2 emissions from MACC-III were scaled (except for Russia, for which the
312 MACC_III emissions were used also in the DT+IVOC runs) to better match the bottom-up inventory
313 ‘DT’ from Denier van der Gon (2015a), where DT refers to data from dilution tunnels, which capture
314 condensables (SVOC) in addition to solid particles. This causes a substantial increase in POA
315 emissions for some countries (e.g. by more than a factor of three for Germany), but only minor for
316 others (e.g. Norway), as discussed by Denier van der Gon, (2015a). The DT/IVOC case adds extra
317 emissions of intermediate volatility compounds (IVOC) for all primary OA (POA) sources, as in
318 Denier van der Gon (2015a). The split between biomass burning (non-fossil) emissions and fossil fuel
319 based emissions for SNAP-2 was taken from the inventory of Denier van der Gon (2015a). Table 3
320 details the volatility assumptions used for the DT+IVOC case. EC emissions from wood combustion
321 are also different in the two different inventories (see Genberg et al., 2013, for a detailed discussion of
322 the EC emissions in the DT emission inventory).

323

324 2. Source apportionment using Latin Hypercube Sampling

325 Source apportionment of TC into different source categories of fossil-fuel, biomass burning and
326 remaining non-fossil carbon for OC and EC has been done with chemical and ^{14}C tracers. This
327 methodology, which is very similar to that used in Yttri et al. (2011a), was originally developed for the
328 CARBOSOL project (Gelencsér et al., 2007), and has been refined over the years, and applied in
329 several Nordic studies (Szidat et al., 2009, Yttri et al., 2011a, b, Glasius et al., 2018). In summary:
330 Measurements of levoglucosan are used as a tracer of wood-burning emissions ($\text{TC}_{\text{bb}} = \text{OC}_{\text{bb}} + \text{EC}_{\text{bb}}$;
331 OC_{bb} includes primary and secondary OC) and the ^{14}C isotopic ratio ($F^{14}\text{C}$), along with measured OC
332 and EC, and assumed emission ratios (e.g. $\text{TC}_{\text{bb}}/\text{levoglucosan}$ and $\text{OC}_{\text{bb}}/\text{TC}_{\text{bb}}$ from wood combustion,
333 or OC/EC ratios from fossil-fuel combustion), to assign the remaining carbon between fossil-fuel
334 sources and secondary organic aerosol sources. When available (as in Yttri et al., 2011a), mannitol and
335 cellulose can be used as tracers of primary biological aerosol particles (OC_{PBAP}) derived from fungal
336 spores (OC_{pbs}) and plant debris (OC_{pbc}), respectively. Total carbon is in this way split into TC_{bb} ,
337 OC_{PBAP} , $\text{TC}_{\text{ff}} (= \text{OC}_{\text{ff}} + \text{EC}_{\text{ff}}$, from fossil-fuel sources; OC_{ff} includes primary and secondary OC), and
338 finally, any remaining modern-carbon is labeled OC_{mf} , which typically is dominated by OC_{BSOA}
339 (biogenic secondary organic aerosol), but might also include other sources, such as SOA from biomass
340 burning and emissions related to cooking (Mohr et al., 2009; Crippa et al., 2014). Note that Crippa et



341 al. (2014) did not find any influence of cooking at European rural background sites doing a source
342 apportionment study of the carbonaceous aerosol based on Aerosol Mass Spectrometer (AMS)
343 measurements. The relationship between any tracer and its derived TC component is very uncertain,
344 thus an uncertainty distribution of allowed parameter values for all important emission ratios or
345 measurement inputs is assigned. In order to solve the system of equations, allowing for the multitude of
346 possible combinations of parameters, an effective statistical approach known as Latin-hypercube
347 sampling is used, which is comparable to Monte Carlo calculations. In brief, central values with low
348 and high limits are associated to all uncertain input parameters. These factors are combined using LHS
349 in order to generate thousands of solutions for the source-apportionment. All valid combinations of
350 parameters (i.e. excluding those producing negative solutions) are condensed in frequency distributions
351 of possible solutions. Extensive discussion of the choices behind the factors used, and their
352 uncertainties, can be found in earlier related studies (Yttri et al., 2011a, Szidat et al., 2009 Gelencsér et
353 al., 2007, Simpson et al., 2007). The result of this analysis consist of so-called central-estimates of the
354 TC components (i.e. the 50th percentile), as well as the range of possibilities allowed by the LHS
355 calculation, e.g. expressed as the 10th and 90th percentiles of the solutions.

356 There are two major differences in the data available for this study compared to Yttri et al.
357 (2011a, b), requiring modification of the methodology and factors used: i) For the present study, we
358 have no data to estimate the fractions of PBAP and BSOA, thus OC_{mf} comprises both OC_{BSOA} , OC_{PBAP}
359 and indeed all other non-fossil sources of OC; ii) The geographical scope of the current study is wider,
360 and in particular biomass burning in southern Europe involves different tree species than those used in
361 the Northern European studies of Yttri et al. (2011a,b) or Szidat et al. (2009).

362 Concerning item (i), we require a range of values of the $F^{14}C$ value associated with OC_{mf} . In
363 Yttri et al. (2011a,b) we used 1.055 for BSOA and PBAP associated with plant debris, but allowed
364 $F^{14}C$ for spores to vary between 1.055 and 1.25, reflecting the utilization of older carbon-stocks by
365 fungi. As noted above, we have no direct tracers for BSOA or PBAP, but a few studies allow a general
366 estimate. Winiwarter et al. (2009) suggested that fungal spores were likely the dominant contributor to
367 PBAP across Europe. Results scaled for Europe indicated a contribution of PBAPs to PM_{10}
368 concentrations in the low percentage range, with a maximum in summer when PM_{10} concentration
369 levels are small. Similarly, Bauer et al. (2008) had spores contributing 6% to OC in spring and 14% in
370 summer at a suburban site, whereas the corresponding contribution to PM_{10} was 3% (spring) and 7%
371 (summer). In Norway, Yttri et al. (2011a) found spores and debris contributing 18% and 6%,
372 respectively, to TC at a rural site in summer, with 0.5% and 7% respectively in winter. For comparison,
373 BSOA contributed 56% and 11% of TC in summer and winter at the actual site. Hence, spores and
374 plant debris are likely to make a certain contribution, but are unlikely to dominate OC_{mf} . In order to
375 account for this, we allow $F^{14}C$ to vary between 1.055 to 1.100 in the present study.

376 Concerning item (ii), the main effect is likely to be on the assumed TC/levoglucosan ratios
377 used in the LHS method. In Yttri et al. (2011a,b) we used low, central and high values of 11, 15 and 17
378 for PM_{10} , or 7.6, 12, and 14 for $PM_{2.5}$, factors derived from ambient Norwegian data, and modified to
379 be appropriate to the QBQ sampling used for the LHS. These values also seem to be consistent with the
380 study of Elsasser et al. (2012), which reported OC/levoglucosan values from filter samples of about



381 10–17 for Augsburg, Germany. Inclusion of EC would give $TC_{bb}/levoglucosan$ values at the high end
382 of our assumed range.

383 We have no equivalent data for southern Europe, but a simple examination of the data in Table
384 2 suggests that levoglucosan levels can be high at the Italian sites, and assuming high ratios of
385 $(TC/levoglucosan)_{bb}$ in emissions would result in LHS-estimated TC_{bb} higher than observed TC, which
386 clearly is impossible. Gilardoni et al., (2011) used $(OC/levoglucosan)_{bb}$ of 4 to 13, then $(OC/EC)_{bb}$ of 1
387 to 20, whereas Zotter et al. (2014) observed $(OC/levoglucosan)_{bb}$ of 7.8 ± 2.7 and $(OC/EC)_{bb}$ of 8.6 ± 2.9
388 for Southern Switzerland, which is close to the Italian site Ispra. It isn't obvious how to derive
389 $(TC/levoglucosan)_{bb}$ from these values, but low values are clearly suggested by these choices.

390 In order to allow for this possibility, we have extended the lower range of our
391 $(TC/levoglucosan)_{bb}$ ratio to be 5, thus using low, central and high of 5, 15 and 17 for PM_{10} . This
392 actually made very little difference to the LHS solutions for central and northern Europe, but allowed
393 more solutions for the Italian sites.

394 No attempts to run LHS were possible for samples with unrealistically high $^{14}C(TC)$ values,
395 affecting two samples each from Birkenes and Košetice. No valid solution was obtained for five of the
396 samples collected at Ispra, two at Melpitz, one at Birkenes and one at Payerne. This may be an
397 indication of problems with the samples (e.g. artefacts or contaminated $^{14}C(TC)$ values), or with the
398 assumptions underlying LHS breaking down. Nevertheless, LHS-based source apportionment was
399 obtained for 29/35 samples in fall and for 29/36 in winter/spring.

400

401 3. Results

402 3.1 Ambient concentrations of the carbonaceous aerosol

403 Concentrations of elemental carbon (EC), positive-artefact-corrected particulate organic carbon (OC_p),
404 organic carbon on back filters (OC_B), positive-artefact-corrected particulate total carbon (TC_p) and
405 levoglucosan, as well as the EC/TC_p ratio and the $f_{nr}(TC_p)$ fraction observed during the fall 2008 and
406 the winter/spring 2009 intensive measurement periods, are presented in Table 2.

407

408 3.1.1 EC and OC_p

409 The mean EC concentration ($0.64 \pm 0.58 \mu\text{g C m}^{-3}$ in fall; $0.58 \pm 0.50 \mu\text{g C m}^{-3}$ in winter/spring) was
410 quite similar to the annual mean concentration reported for 12 European rural background (EMEP)
411 sites in 2002–2003 ($0.66 \pm 0.39 \mu\text{g m}^{-3}$; Yttri et al., 2007a), but slightly less than the winter time mean
412 ($0.79 \pm 0.83 \mu\text{g C m}^{-3}$; *ibid.*). Although thermal-optical analysis was used both in the present study and
413 in that by Yttri et al. (2007a), different temperature protocols can cause substantial differences in the
414 OC/EC split. However, only a minor difference was observed with respect to the EC/TC ratio when
415 analyzing the “8785 Air Particulate Matter On Filter Media” reference material from NIST using the
416 EUSAAR-2 protocol and the NIOSH derived protocol (Yttri et al., 2007a). The mean EC concentration
417 varied by a factor of ~15 between sites both in fall and in winter/spring, with concentrations at
418 Birkenes and Mace Head (North-western Europe) being substantially lower than for continental
419 European sites, particularly compared to the southern sites (Montelibretti, Ispra and K-puszt). A
420 pronounced North-to-South gradient for EC, and OC, has previously been reported by Yttri et al.



421 (2007a), reflecting diluted emissions from major source regions in continental Europe reaching distant
422 and less polluted sites on the outskirts of Europe. In addition, the proximity to the coast causes efficient
423 ventilation and air mass mixing at the sites Birkenes and Mace Head.

424 The mean OC_p concentrations in fall ($2.9 \pm 3.1 \mu\text{g C m}^{-3}$) and winter/spring ($2.8 \pm 2.3 \mu\text{g C m}^{-3}$)
425 were almost identical. A few, high concentration samples at the sites Montelibretti, Ispra and K-puszt
426 influenced the winter/spring mean, as evident from the mean-to-median ratio of 1.6 compared to 1.2 in
427 fall. Mean OC_p concentrations reported here were slightly lower than the annual ($3.4 \pm 3.6 \mu\text{g C m}^{-3}$) and
428 winter time ($3.7 \pm 4.4 \mu\text{g C m}^{-3}$) mean OC concentrations reported for EMEP sites in 2002–2003 (Yttri
429 et al., 2007a). Differences in sampling time, temperature protocol, and sampling approach [the current
430 study accounted for the positive sampling artefact of OC, whereas Yttri et al., (2007) did not], are
431 likely to explain the (minor) differences in the OC concentration between the two studies. If we allow
432 for a positive artefact of similar magnitude as that observed in the present study, $16 \pm 8 \%$ in fall and
433 $17 \pm 9 \%$ in winter/spring, also for the Yttri et al. (2007a) study, levels would be fairly similar.

434 A North-to-South gradient was observed for OC_p as for EC, which was less prominent in fall
435 compared to winter/spring.

436

437 3.1.2 EC/TC ratio

438 The EC/ TC_p ratio ranged from 11 to 28 % in fall, and from 14 to 24 % in winter/spring. No pronounced
439 shift in the EC/ TC_p ratio was observed between the two periods, except for the Norwegian site
440 Birkenes, for which the EC/ TC_p ratio was 11% in fall and 21% in winter/spring.

441

442 3.1.3 Levoglucosan

443 The mean concentration of the wood burning tracer levoglucosan varied by more than a factor of 50
444 between sites, both in fall and in winter/spring. There was a pronounced North-to-South gradient, as for
445 OC_p and EC and the mean concentration was higher in winter/spring than in fall at all sites, except
446 Košetice and Mace Head. The levoglucosan level is within the range reported for six European rural
447 background sites (2.7 – 1220 ng m^{-3}) by Puxbaum et al. (2007), and for Montelibretti, Ispra, and K-
448 puszt, levels equaled the concentration range reported for urban areas in winter (Szidat et al., 2009).

449



450 3.1.4 $f_{\text{nf}}(\text{TC}_p)$ from ^{14}C analysis

451 The non-fossil fraction of TC_p (i.e. $f_{\text{nf}}(\text{TC}_p)$) of individual aerosol filter samples varied from 0.51 to
452 >1.00 . Two samples from Birkenes and two samples from Košetice showed such high $^{14}\text{C}(\text{TC})$ results
453 that the corresponding $f_{\text{nf}}(\text{TC}_p)$ resulted in levels as high as 1.68. These unreasonable values point to an
454 anthropogenic bias of local ^{14}C emissions, which distort the source apportionment. Similar cases have
455 occasionally been observed at other sites, mainly caused by local pharmaceutical facilities with
456 incineration units for ^{14}C -labelled waste (Buchholz et al., 2013; Zotter et al., 2014). In some cases, the
457 specific source could not be identified, as for Birkenes and Košetice. Consequently, the biased values
458 were excluded from further analysis. The remaining results from these two sites were included, as they
459 correspond well with values from the other sites, although their reliability remains unclear.

460 Mean $f_{\text{nf}}(\text{TC}_p)$ values ranged from 0.61–0.91 for the individual sites, including both fall and
461 winter/spring. These values correspond to those reported at five European rural and remote sites in
462 summer and winter by Gelencsér et al. (2007) and to an urban and a rural site in Norway (Yttri et al.,
463 2011a), but are higher compared to rural and urban sites in Switzerland and Sweden during summer
464 and winter (Szidat et al., 2009). The seasonal variation was typically not pronounced, although most
465 sites experienced the highest $f_{\text{nf}}(\text{TC}_p)$ values in winter/spring. The exceptions were Montelibretti, at
466 which $f_{\text{nf}}(\text{TC}_p)$ was noticeably higher in winter/spring (0.80) compared to fall (0.61), and Košetice at
467 which $f_{\text{nf}}(\text{TC}_p)$ was higher in fall 2008 (0.86) compared to winter/spring 2009 (0.69).

468

469 4. Discussion

470 Results from the carbonaceous aerosol source apportionment (Figure 2; Table 4) show a variability in
471 the carbonaceous aerosol source composition, both as a function of season and location. The results
472 from the source apportionment analyses are discussed in detail in sections 5.1–5.5. Calculated
473 concentrations and relative contributions typically showed little variability between samples collected
474 within each season for each of the nine sites. Hence, comparing results based on calculated mean
475 values can be argued for. The results presented are complementary to those of Gelencsér et al. (2007),
476 Genberg et al. (2011) and Yttri et al. (2011a,b), as the same same (or similar in the case of Genberg et
477 al.) software/methodology is applied, but for a wider range of sites, and with updated emission ratios
478 (Zotter et al., 2014) for the central and southern European sites.

479

480 4.1 Carbonaceous aerosol from fossil-fuel sources and biomass burning

481 Fossil fuel combustion was the major source of EC at all sites in fall, accounting for 6% to 22% of TC_p ,
482 whereas EC from biomass burning was $< 8\%$ at all sites. The influence of EC_{ff} was particularly
483 pronounced at the sites Montelibretti (22%) and Lille Valby (21%), which for Montelibretti could be
484 due to the proximity of the Rome metropolitan area, with 3.7 million inhabitants. Lille Valby is a semi-
485 rural site, and thus could be more influenced by e.g. vehicular particulate emissions. Fossil fuel
486 combustion continued to be the most important source of EC in winter/spring for the five northernmost
487 sites, whereas there was a shift towards biomass burning for the four southernmost sites. The relative
488 contribution of EC_{bb} and EC_{ff} to TC_p in winter/spring was $\leq 10\%$, except at the sites Lille Valby,
489 Melpitz and Birkenes that experienced relative contributions of EC_{ff} exceeding 10%. EC_{bb} was a more



490 abundant fraction of TC_p in winter/spring compared to fall at all sites. The picture was less consistent
491 for EC_{fr} , with a higher relative contribution in fall at the four southernmost sites, and for Lille Valby,
492 and a higher fraction in winter/spring for the four other sites.

493 Biomass burning was the major anthropogenic source of OC at most sites in fall, accounting
494 from 5% to 36% of TC_p , whereas OC from fossil fuel ranged from 8% to 21%. The exceptions were
495 Birkenes and Mace Head for which OC_{fr} dominated with 16% and 21%, respectively. At Montelibretti,
496 OC_{bb} and OC_{fr} made equally large contributions to TC_p (18% each).

497 In winter/spring, biomass burning was the major anthropogenic source of OC at all sites
498 except at Mace Head, constituting 11% to 46% of TC_p , whereas the range for OC_{fr} was 10% to 23%.
499 OC_{bb} was more abundant in winter/spring compared to fall for all sites but Mace Head, whereas there
500 was no consistent pattern observed for OC_{fr} . There was a general tendency that OC_{bb} became less
501 abundant along a South-to-North transect, as seen for EC_{bb} .

502 Biomass burning had a pronounced influence at most sites already in the first week of
503 sampling in fall (17–24 September): EC_{bb} and OC_{bb} contributed a substantial 57% of TC_p at K-pusztá
504 and 54% at Ispra, 34% and 37% at Melpitz and Payerne, respectively, whereas it ranged from 21–29%
505 for the sites Mace Head, Košetice and Lille Valby. Birkenes was the only sites where wood burning
506 made a minor contribution (6%) this week. Model calculations suggest that wild and agricultural fires
507 were of minor importance at all sites for the actual week, with the highest model calculated
508 concentration ($0.02 \mu\text{g C m}^{-3}$) at Ispra and Lille Valby, corresponding to 3% and 5% of the modelled
509 TC_{bb} (See section 5.2). Hence, residential wood burning appears to be the source of EC_{bb} and OC_{bb} ,
510 although given the uncertainties of emission estimates for wild and agricultural fires, such sources
511 cannot be ruled out. The mean temperature during the first week of sampling was not noticeably lower
512 than seen for the rest of the sampling period. Still, it was the week with the lowest mean temperature
513 for the sites K-pusztá, Payerne and Košetice.

514

515 4.2 Wild and agricultural fire contribution

516 Wild and agricultural fires are major sources of carbonaceous aerosol (Bond et al., 2004), but with
517 large regional, seasonal and annual differences in emissions and occurrence (Hao et al., 2016; Korontzi
518 et al., 2006). Agricultural waste burning is banned in most European countries, as it is a major source
519 of forest fires, and thus a threat to human life and properties, as well as a source of severe air pollution.
520 Nevertheless, remote sensing data show such fire events in several countries, including those with a
521 ban (Korontzi et al., 2006), and it appears particularly frequent in Eastern Europe (e.g. Belarus and the
522 Ukraine), in western parts of Russia and in Central Asia. In most cases when natural vegetation catches
523 fire in Europe, this is due to human activity (Winiwarter et al., 1999).

524 Incidences of wild and agricultural fires that severely deteriorate air quality in large parts of
525 Europe are regularly reported e.g. by Yttri et al. (2007a) for 2002, by Stohl et al. (2007) for 2006, and
526 Diapouli et al. (2014) for 2010. The two periods discussed in the present study partly coincide with the
527 time when concentrations from wild and agricultural fires peak in Europe (Korontzi et al., 2006).
528 Levoglucosan by itself cannot differentiate between emissions from residential wood burning and wild
529 and agricultural fires. Hence, we have used modelled concentrations to address the relative contribution



530 of TC from wild fires and agricultural fires (TC_{wf}) to the sum of TC from residential wood burning
531 (TC_{bb}) and TC_{wf} for the two sampling periods.

532 There was an influence from wild and agricultural fires at all sites, with a higher mean
533 contribution in fall ($TC_{wf} = 0.05 \mu\text{g C m}^{-3}$), corresponding to 9–16% (for base-case, or DT+IVOC) of
534 modelled TC_{bb} , than in winter/spring ($TC_{wf} = 0.015 \mu\text{g C m}^{-3}$), corresponding to 2–4% of modelled
535 TC_{bb} . TC_{wf} were typically low also on a weekly basis, but for the last week of sampling in fall, a
536 noticeable contribution was calculated for Ispra (34%), K-pusztá (31%), and Montelibretti (16%).

537 The major conclusion to be drawn from these results is that the model predicts that wild and
538 agricultural fires make minor contributions to the biomass burning carbonaceous aerosol at the sites
539 addressed, and that residential wood burning is the major source.

540

541 4.3 Remaining non-fossil sources of organic carbon

542 Remaining non-fossil sources of OC (OC_{mf}) are typically associated with biogenic secondary organic
543 aerosol (OC_{BSOA}) and primary biological aerosol particles (OC_{PBAP}), however there are anthropogenic
544 sources of modern carbon as well, as discussed in detail by Yttri et al. (2011a). Here, we discuss the
545 results obtained for OC_{mf} as if natural sources are dominating.

546 The OC_{mf} level varied more widely in winter ($0.1\text{--}2.2 \mu\text{g C m}^{-3}$) than in fall ($0.6\text{--}3.0 \mu\text{g C m}^{-3}$)
547 (Figure 2) and corresponds well with levels reported for the European rural background environment
548 (Gelencsér et al., 2007; Genberg et al., 2011; Yttri et al., 2011a,b). The spatial distribution of OC_{mf}
549 equaled that of OC_p , with high concentrations at the southernmost sites and decreasing levels along a
550 South-to-North transect.

551 OC_{mf} levels were higher in fall compared to winter/spring for all sites, but the difference
552 varied from minor at most sites, moderate at the continental sites Košetice and Payerne, and substantial
553 at the Norwegian site Birkenes. Studies consistently point towards BSOA as the major contributor to
554 OC_{mf} in Europe (e.g., Simpson et al., 2007; Bessagnet et al., 2008; Yttri et al., 2011a); e.g. Gelencsér et
555 al. (2007) showed that BSOA in $PM_{2.5}$ was 1.6–12 times higher in summer than in winter for six
556 European rural background sites. Hence, the observed pattern could partly be explained by a higher
557 formation rate of BSOA in fall, propelled by larger emissions of BSOA precursors and a higher
558 ambient temperature (See Table 1 ambient temperature values). In the present study, PM_{10} filter
559 samples were collected (except at Mace Head, where $PM_{2.5}$ was collected). Consequently, primary
560 biological aerosol particles (PBAP), typically residing in the coarse fraction of PM_{10} (e.g., Yttri et al.,
561 2007b; Kourchev et al., 2009; Bozzetti et al., 2016), could contribute to OC_{mf} as well. In Scandinavia,
562 PBAP peak in summer and fall, reflecting the vegetative season and the absence/presence of a snow
563 cover (Yttri et al., 2007a,b; 2011a,b), and summer time OC_{PBAP} concentrations (PM_{10}) being 7–8 times
564 higher than in winter, has been reported for two Norwegian sites (Yttri et al., 2011a). In continental
565 Europe, the vegetative season is longer than in Scandinavia and a permanent snow cover is associated
566 with high altitude regions and rare occasions, lasting for short periods, in low altitude regions. Hence,
567 one could speculate that there is a PBAP emission flux in continental Europe in the heating season,
568 which is comparatively larger than that observed in Scandinavia. We find support of this view in the
569 study by Waked et al. (2014), which showed a tail of PBAP and episodes with high PBAP



570 concentrations in winter for an urban background site in Northern France. Knowledge of PBAP
571 concentrations in Europe is limited, thus we can only speculate about how much of OC_{mf} in the present
572 study is due to PBAP. A noticeable 20–32% contribution of OC_{PBAP} to TC_p was found at four Nordic
573 rural background sites in late summer (Yttri et al., 2011b). Similar figures (OC from primary biogenics
574 constituting up to 33% of OC in PM_{10}) were reported for the densely populated region of Berlin in
575 north-eastern Germany (Wagener et al., 2012) in late summer and fall. Gelencsér et al. (2007) and
576 Gilardoni et al. (2011) both reported levels of OC associated with PBAP for an entire year for the
577 European rural background environment, finding that the relative contribution to total carbon was < 5%
578 in summer and < 8% in winter. However, both studies relied on $PM_{2.5}$ samples, likely excluding the
579 majority of PBAP. Further, Gelencsér et al. (2007) accounted for plant debris only when measuring
580 cellulose, whereas Gilardoni et al. (2011) only accounted for fungal spores, measuring
581 arabitol/mannitol. Waked et al. (2014) found that 17% of the OC was attributed to OC_{PBAP} on an annual
582 basis for an urban background site, with substantially higher concentrations in summer (37%) and fall
583 (20%) compared to winter (7%) and spring (6%). At the rural background site Payerne, Bozzetti et al.
584 (2016) found that PBAP, mainly from plant debris, equaled the contribution of SOA to organic matter
585 in PM_{10} in summer.

586 The non-fossil signal was typically most pronounced in fall, with the highest relative share (52 –
587 69%) observed for the two low loading sites situated on the outskirts of Europe (Birkenes and Mace
588 Head) and the lowest for the highest loading site, Ispra (23%). A pronounced non-fossil signal (52 –
589 54%) was seen for the continental sites Košetice and Payerne as well, whereas the relative share ranged
590 between 38% and 48% for the remaining sites. Non-fossil OC was by far the major source of OC at all
591 sites in fall, except at Ispra, for which biomass burning dominated. The non-fossil signal decreased, or
592 remained unchanged, for all but one site going from fall to winter/spring, but the reduction was
593 substantial only at the Norwegian site Birkenes (a factor of ~2), at Payerne and Košetice (a factor of
594 1.5–1.7), and at Melpitz (a factor of 1.5). Still, non-fossil OC was the major source of OC at five sites
595 even in winter/spring, K-pusztá, Košetice, Lille Valby, Mace Head and Birkenes. It has been suggested
596 that increased condensation due to lower temperatures could be an efficient way of forming BSOA
597 even in winter (Simpson et al., 2007). It is however difficult to argue for such a hypothesis barely by
598 looking at the observed ambient air temperatures during the winter/spring period. Another possibility is
599 that some of the remaining non-fossil OC may be secondary organic aerosol formed from volatile or
600 semi-volatile OC emitted from wood burning. OC_{bb} determined based on levoglucosan may not include
601 all SOA formed after aging of the gas-phase emissions, even if the emission ratios were derived from
602 ambient measurements and likely include condensed vapors and secondary products.

603

604 4.4 Natural versus anthropogenic sources of carbonaceous aerosol

605 In the current study, results obtained for OC_{mf} are discussed as if natural sources are dominating,
606 despite that anthropogenic sources can make a certain contribution, e.g. from cooking emissions and by
607 anthropogenic enhancement of BSOA formation. EC and OC emitted from combustion of fossil fuel
608 and biomass are considered entirely anthropogenic, as we define wild fires as anthropogenic.



609 In fall, the anthropogenic and natural influences were of comparable magnitude at most sites.
610 Exceptions were Birkenes, with a clearly larger natural contribution (69%), and Ispra, with a larger
611 anthropogenic contribution (77%), the latter affected by regional air pollution in the strongly polluted
612 Po Valley region. For the other sites, the anthropogenic fraction ranged from 46 – 62% and from 38 –
613 54% for the natural fraction. Increased condensation due to lower temperatures can be an important
614 source of BSOA in fall and winter, which could outweigh the effect of high temperature and increased
615 terpene emissions in summer (Simpson et al., 2007). Further, PBAP can make a pronounced
616 contribution in fall both in Scandinavia (Yttri et al., 2007a,b; 2011a,b) and in continental Europe
617 (Waked et al., 2014; Bozzetti et al., 2016), and the fall peak of the North-Eastern Atlantic Ocean
618 phytoalgal bloom takes place during the period in question, likely contributing with marine PBAP at
619 Mace Head (Ceburnis et al., 2011).

620 In winter/spring, anthropogenic sources dominated at all sites (60 – 78% anthropogenic),
621 except for Mace Head (37%). Ispra had the most pronounced anthropogenic contribution of all sites
622 also in winter/spring (78%), and it was largely unchanged from that observed in fall. Three of the four
623 sites experiencing a high natural influence in fall, (Birkenes, Košetice and Payerne) saw a major
624 increase in the anthropogenic contribution going from fall to winter/spring. This was attributed to a
625 substantial reduction in natural sources, accompanied by an increase in the anthropogenic sources,
626 being primarily biomass burning at Payerne and Birkenes and fossil fuel sources at Košetice.
627 Residential wood burning is considered a decentralized source in Europe, and emissions from local
628 sources can be substantial in winter (Szidat et al., 2007). A certain local contribution could also be
629 speculated for Košetice, as small coal-fired ovens still are common in rural areas in Eastern Europe
630 (Spindler et al., 2012).

631

632 4.5 Modelling contributions from biomass burning

633 The EMEP MSC-W model was run with two different emission and SOA modelling set-ups (a base-
634 case and DT+IVOC) in order to reflect (to some extent) the very large uncertainties in both emissions
635 and atmospheric processing of the primary organic aerosol (POA) (see section 2.7). The model results
636 were compared with that of the LHS analysis discussed above. In the following, model results that are
637 within the 10–90 percentile range of the LHS analysis are considered as being in “agreement” with the
638 measurements. Results outside this (fairly wide) concentration range are considered as under or over
639 estimations.

640 Modelled OC_{bb} and EC_{bb} concentrations were compared to the LHS source apportionment
641 results for each sample individually in Figure 3, and as averages over the measurement periods in Table
642 4. The base-case model simulations underestimated OC_{bb} severely at most sites (Figure 3a). The only
643 exception was Birkenes, for which the model slightly overestimated the LHS-derived estimates (the
644 modelled OC_{bb} were within the LHS 10–90 percentile range for 3/5 weeks, whereas 2/5 weeks were
645 overestimated). For the other sites, the mean underestimation of the LHS 10-percentile for OC_{bb} ranged
646 from –26% at Lille Valby to –84% at Payerne.

647 The model results for OC_{bb} were clearly better with the DT+IVOC emission set-up (Figure
648 3b), than for the base-case, at all sites except Birkenes and Lille Valby. For Košetice and Payerne, the



649 modelled OC_{bb} was within the LHS range for a majority of the samples and the underestimation of
650 OC_{bb} was smaller than with the base-case for Ispra, Montelibretti, K-pusztá and Melpitz. A few
651 individual OC_{bb} measurements were, however, clearly overestimated with the DT+IVOC setup (one
652 sample each for Melpitz, K-pusztá and Lille Valby).

653 The results for EC_{bb} roughly split in two groups for the base-case (Figure 3c): At Birkenes and
654 Lille Valby, the EC_{bb} concentrations were overestimated by the model most of the time; only for one
655 sample at each site did the model EC_{bb} fall within the LHS-range. The average overestimation of the
656 LHS 90-percentile was 69% at Lille Valby and 43% at Birkenes. At the other sites, EC_{bb} was
657 underestimated (with a few exceptions), with an average underestimation ranging from -34%
658 compared to the LHS 10-percentile at Melpitz to -84% at Mace Head. For the two Italian sites the
659 average underestimation was -38%, whereas it was -39% at K-pusztá and Košetice and -60% at
660 Payerne.

661 The DT+IVOC model results were clearly better for EC_{bb} , except for the Italian sites and K-
662 pusztá where the EC_{bb} underestimation was larger due to lower
663 emissions in the inventory of Denier van der Gon et al. (2015a). EC_{bb} was largely overestimated at the
664 Scandinavian sites, but not as much as for the base-case emissions. The modelled EC_{bb} was within the
665 10–90 percentile LHS range for five of the weeks at Košetice and Payerne using the DT+IVOC
666 emissions, but there was still a tendency that levels were underestimated (one week was underestimated
667 at Košetice, two at Payerne). For Melpitz the modelled EC_{bb} was within the LHS range for 3/6 weeks
668 (two weeks were underestimated and one overestimated).

669 The present comparison of modelled and LHS-derived biomass burning carbonaceous aerosol
670 concentrations, indicates that the base-case setup with the TNO MACC-III emission inventory, which
671 is similar to official EMEP $PM_{2.5}$ emissions estimates, likely underestimates emissions from residential
672 wood burning substantially in large parts of Europe. This is in line with the findings of Denier van der
673 Gon (2015a), and reflects that emissions are established following national practice that is inconsistent
674 between countries. Note that the inventory POA emissions were distributed across different volatility
675 classes for the DT+IVOC emissions, as for a typical VBS treatment, whereas we did not add IVOC to
676 the MACC-III emissions in our base-case. Although the DT+IVOC emission setup with updated wood
677 burning emissions and extra IVOC improved the model results, large uncertainties still remain, and it
678 cannot be excluded that wood burning emissions in some parts of Europe may be considerably larger
679 than that estimated by Denier van der Gon et al. (2015a).

680

681 5 Conclusions

682 Source apportionment of carbonaceous aerosol was conducted at nine European rural background sites
683 for a fall period in 2008 and a winter/spring period in 2009. The approach separated the carbonaceous
684 aerosol into a natural and an anthropogenic fraction, and divided the anthropogenic fraction into fossil
685 fuel and biomass burning origin, which is a prerequisite for targeted abatement strategies. The fraction
686 apportioned to biomass burning was compared with calculated concentrations using the EMEP model,
687 applying a base-case and an alternative emission set up with intermediate volatility compounds
688 (IVOC).



689 The total carbonaceous aerosol concentration, as well as the carbonaceous aerosol apportioned
690 to biomass burning, fossil fuel and natural sources, decreased from South to North. Natural sources
691 typically accounted for a larger fraction of the carbonaceous aerosol in fall compared to winter/spring,
692 likely because the fall sampling period partly took place in the vegetative season. The seasonal
693 differences of the natural sources varied from minor at most sites, moderate at two of the continental
694 sites, to substantial at the northernmost Scandinavian site. Biomass burning aerosol had an opposite
695 seasonal behavior to that of natural sources, following the increased emissions from residential wood
696 burning in the heating season. No consistent seasonal pattern was observed for fossil fuel aerosol and
697 their contribution to the carbonaceous aerosol, possibly because domestic heating is a minor source of
698 fossil fuel carbon compared to e.g. vehicular traffic.

699 Anthropogenic sources (60–78%) dominated at all but the most remote site in winter/spring,
700 and residential wood burning (36–56%) was typically the major anthropogenic source of TC. In fall,
701 anthropogenic and natural influence were of comparable magnitude at most sites, except at Birkenes
702 (69% natural) and Ispra (77% anthropogenic). Biomass burning was the major anthropogenic source at
703 Central European sites in fall (29–44%), whereas fossil fuel dominated at the southernmost (40%) and
704 the three northernmost sites (29–37%).

705 Model calculated concentrations of carbonaceous aerosol from biomass burning were severely
706 underestimated, except for the Scandinavian sites, when using the base-case MACC-III emission
707 inventory. Model results improved when an alternative bottom-up approach with added IVOC was
708 used. However, OC_{bb} and EC_{bb} levels were still substantially underestimated at the southernmost sites.

709 The current study shows that natural sources are major contributors to the carbonaceous
710 aerosol at background sites in Europe even in fall and in winter/spring, and that residential wood
711 burning emissions can be equally large or larger than that of fossil fuel sources, depending on season
712 and region. Our results suggest that residential wood burning emissions are poorly constrained for large
713 parts of Europe and that the need to improve emission inventories is obvious, with harmonized
714 emission factors between countries likely being the most important step to improve model calculations.
715 Revised wood burning emissions will also improve model predictions of $PM_{2.5}$ concentrations in
716 Europe, particularly in the heating season. EMEP intensive measurement periods are essential for real-
717 world evaluation of model results, especially when the underlying emission data are so uncertain; as is
718 future EMEP intensive measurement periods targeted on the wood burning source.

719
720 *Author Contributions.* KEY was responsible for the main design, coordination of the study, the
721 synthesis of the results, writing most of the paper, responsible for the centralized analysis of
722 levoglucosan, and provide OC/EC data for Birkenes. DS did the Latin Hybercube Sampling (LHS), as
723 well as the EMEP modelling part together with RB. DS wrote the text on LHS, whereas DS and RB
724 together wrote the text on the modelling, as well as they thoroughly reviewed the paper. GK wrote the
725 introduction, provided OC/EC data for K-pusztá and wrote the description of the site, and thoroughly
726 reviewed the paper. SS and Y-LZ were responsible for and performed the centralized ^{14}C -analysis,
727 wrote the text on this topic, and thoroughly reviewed the paper. WAA and ASHP contributed to the
728 coordination of the study and thoroughly reviewed the paper. CH provided OC/EC data for Payerne,



729 wrote the description of the site and thoroughly reviewed the paper. CP provided OC/EC data for
730 Montelibretti, wrote the description of the site and thoroughly reviewed the paper. DC provided OC/EC
731 data for Mace Head, wrote the description of the site and thoroughly reviewed the paper. GS provided
732 OC/EC data for Melpitz, wrote the description of the site and thoroughly reviewed the paper. JPP
733 provided OC/EC data for Ispra, wrote the description of the site and thoroughly reviewed the paper.
734 JKN provided OC/EC data for Lille Valby and wrote the description of the site. MV provided OC/EC
735 data for Košetice and wrote the description of the site. SE and IP thoroughly reviewed the paper.

736

737 *Competing interests.* The authors have no conflict of interest.

738

739 *Acknowledgements.* This work was supported by the Co-operative Programme for Monitoring and
740 Evaluation of the Long-range Transmission of Air pollutants in Europe (EMEP) under UNECE, the
741 European Union Seventh Framework Programme (FP7/2007–2013) under the ACTRIS project (Grant
742 agreement #262254), and the European Union Seventh Framework Programme (FP7/2007–2013)
743 under the ECLIPSE project Grant agreement #282688 – ECLIPSE. Computer time for EMEP model
744 runs was supported by the Research Council of Norway through the NOTUR project EMEP
745 (NN2890K), and this work was also supported by the Swedish Strategic Research Project MERGE
746 (www.merge.lund.se). We are grateful to the Laboratory of Ion Beam Physics of ETH Zurich for
747 providing the accelerator mass spectrometer MICADAS for ¹⁴C measurements. We thank ECMWF and
748 met.no for granting access to ECMWF analysis data. Hugo Denier van der Gon and Jeroen Kuenen
749 from TNO are acknowledged for useful discussions and data concerning OM emissions.

750

751 **APPENDIX A**752 **Detailed description of measurement sites**

753 The Montelibretti EMEP station is situated in central Italy (42°06'N, 12°38'E, 48 m asl) 45 km
754 from the coast of the Tyrrhenian sea. Most of the land surrounding the station are meadows and low
755 intensity agricultural areas. The nearest village (Monterotondo, 30 000 inhabitants) is situated
756 approximately 5 km from the station, whereas the City of Rome lies 20 km to the south-west. Transport
757 of air masses from the urban area of Rome is typically associated with sea-breeze taking place in the
758 early afternoon.

759 The Ispra station (45° 49'N, 8° 38'E, 209 m asl) is situated on the edge of the Po Valley in the
760 north-western part of Italy and is representative for the regional background of this densely populated
761 part of Italy. Major anthropogenic emission sources are situated > 10 km from the site, with the city of
762 Milan, 60 km to the south-east, as the most pronounced one. According to Henne et al. (2010), Ispra
763 is categorized as a typical background site in an environment generally strongly affected by
764 anthropogenic emissions.

765 The Payerne measurement station (46°48'N, 6°56'E, 489 m asl) is part of the Swiss national air
766 pollution monitoring network as well as the EMEP monitoring network, and is regarded as a rural site.
767 The station is located one kilometre south-east of the small town of Payerne (8 000 inhabitants). The
768 site is surrounded by agricultural land (grassland and crops), forests and small villages. The nearest
769 larger cities are Fribourg (15 km east, 35 000 inhabitants), Bern (40 km north east, 125 000 inhabitants)
770 and Lausanne (40 km south-west, 120 000 inhabitants).

771 The K-puszta station (46°58'N, 19°33'E, 130 m asl) is situated in a forest clearing on the
772 Great Hungarian Plain and is representative for the Central-Eastern European regional background
773 environment. The vegetation is dominated by coniferous wood (60%), but also deciduous wood (30%)
774 and grassland are present. The nearest city (Kecskemét) is situated ca 15 km to the SE of K-puszta. The
775 station is part of the Global Atmospheric Watch (GAW) network, the European Monitoring and
776 Evaluation Programme (EMEP) and is also a EUSAAR supersite. The climate is typically continental
777 with low temperatures in winter, mild in spring and fall, and hot and sunny in summer.

778 The Košetice observatory (49°35'N, 15°05'E, 534 m asl) is a joint EMEP and GAW site
779 located in the Czech-Moravian Highlands, approximately 80 km southeast from Prague. Air samples
780 collected at the observatory represents the background level of air quality in the Czech Republic.
781 Forests dominated by conifer trees account for approximately 50% of the land use in the vicinity of the
782 site; the remaining 50% is attributed to meadow (25%) and agricultural areas (25%). The nearest city
783 (Pelhřimov, 15 000 inhabitants) is located 25 km south of the station. The prevailing wind direction is
784 westerly.

785 The Melpitz research station (51°32' N, 12°54' E, 87 m asl) is located on a flat meadow
786 surrounded by agricultural land near the river Elbe. The major city Leipzig is situated 41 km to the
787 south west of the site. Forested areas are located no closer than 1 km from the site. The two dominating
788 wind directions are south west to west, which brings air masses from the Atlantic that passes across
789 Western Europe, and east to south-east, which brings air masses from source regions such as Poland,
790 Belarus, Ukraine and the north of the Czech Republic.



791 The Mace Head atmospheric research station (53°19'N, 9°53'W, 15 m asl) is a GAW supersite
792 situated on the west coast of Ireland, facing the North Atlantic Ocean. The station is located 100 m
793 from the coastline and is surrounded by bare land (rocks, grass and peat bog). A few scattered single
794 houses are located at a distance of 1 km or further away. The nearest city (Galway, 80 000 inhabitants)
795 is located 60 km to the east/south-east of the station. The site experience clean marine air masses from
796 the western sector nearly 50% of the time, whereas polluted air masses are associated with atmospheric
797 transport from UK and continental Europe.

798 Lille Valby (55°41' N, 12°07' E, 12 m asl) is a semi-rural monitoring station in the Sjælland
799 region of Denmark, which has a humid continental climate. The surrounding area is characterized by
800 agricultural land, small villages and the Roskilde Fjord (1 km west of the monitoring site). The station
801 is located 30 km to the west of Copenhagen (1.2 million inhabitants), and 7 km North-East of central
802 Roskilde (46 000 inhabitants). The nearest major road (A6) is located about 800 m west of the station.

803 The Birkenes atmospheric research station (58°23'N, 8°15'E, 190 m asl) is a joint supersite
804 for EMEP and GAW situated approximately 20 km from the Skagerrak coast in southern Norway. The
805 station is located in the boreal forest with mixed conifer and deciduous trees accounting for 65% of the
806 land use in the vicinity of the site; the remaining 35% is attributed to meadow (10%), low intensity
807 agricultural areas (10%), and freshwater lakes (15%). The nearest city (Kristiansand, 65 000
808 inhabitants) is located 25 km south/south-west of the station, and is known to have minor or even
809 negligible influence on the air quality at the site.

810

811 **References**

- 812 Aas, W., Tsyro, S., Bieber, E., Bergström, R., Ceburnis, D., Ellermann, T., Fagerli, H., Frölich, M.,
813 Gehrig, R., Makkonen, U., Nemitz, E., Otjes, R., Perez, N., Perrino, C., Prévôt, A. S. H., Putaud, J.-P.,
814 Simpson, D., Spindler, G., Vana, M., and Yttri, K. E.: Lessons learnt from the first EMEP intensive
815 measurement periods, *Atmos. Chem. Phys.*, 12, 8073-8094, doi:10.5194/acp-12-8073-2012, 2012.
- 816
817 Andreae, M. O. and Ramanathan, V.: Climate's dark forcings, *Science*, 340, 280–281, 2013.
818
819 Bauer, H., Schueller, E., Weinke, G., Berger, A., Hitzemberger, R., Marr, I. L., and Puxbaum, H.:
820 Significant contributions of fungal spores to the organic carbon and to the aerosol mass balance of the
821 urban atmospheric aerosol, *Atmos. Environ.*, 42, 5542–5549, 2008.
- 822
823 Bell, M. L., Ebisu, K., Peng, R. D., Samet, J. M., and Dominici, F.: Hospital Admissions and Chemical
824 Composition of Fine Particle Air Pollution, *Am. J. Resp. Crit. Care*, 179, 1115–1120,
825 doi:10.1164/rccm.200808-1240OC, 2009.
- 826
827 Bergström, R., Denier van der Gon, H. A. C., Prévôt, A. S. H., Yttri, K. E., and Simpson, D.:
828 Modelling of organic aerosols over Europe (2002–2007) using a volatility basis set (VBS) framework:
829 application of different assumptions regarding the formation of secondary organic aerosol, *Atmos.*
830 *Chem. Phys.*, 12, 8499-8527, doi:10.5194/acp-12-8499-2012, 2012.
- 831
832 Bergström, R., Hallquist, M., Simpson, D., Wildt, J., and Mentel, T. F.: Biotic stress: a significant
833 contributor to organic aerosol in Europe? *Atmos. Chem. Phys.*, 14, 13643-13660, 2014.
- 834
835 Bessagnet, B.; Menut, L.; Curci, G.; Hodzic, A.; Guillaume, B.; Liousse, C.; Moukhtar, S.; Pun, B.;
836 Seigneur, C. & Schulz, M. Regional modeling of carbonaceous aerosols over Europe-focus on
837 secondary organic aerosols *J. Atmos. Chem.*, 61, 175-202, 2008.
- 838
839 Birch, M. E. and Cary, R. A.: Elemental carbon-based method for monitoring occupational exposures
840 to particulate diesel exhaust, *Aerosol Sci. Tech.*, 25, 221-241, 1996.
- 841
842 Bond, T. C., D. G. Streets, K. F. Yarber, S. M. Nelson, J.-H. Woo, and Z. Klimont. A technology-based
843 global inventory of black and organic carbon emissions from combustion, *J. Geophys. Res.*, 109,
844 D14203, doi:10.1029/2003JD003697, 2004.
- 845
846 Bond, T. C., Doherty, S. J., Fahey, D. W., Forster, P. M., Berntsen, T., DeAngelo, B. J., Flanner, M. G.,
847 Ghan, S., Kärcher, B., Koch, D., Kinne, S., Kondo, Y., Quinn, P. K., Sarofim, M. C., Schultz, M. G.,
848 Schulz, M., Venkataraman, C., Zhang, H., Zhang, S., Bellouin, N., Guttikunda, S. K., Hopke, P. K.,
849 Jacobson, M. Z., Kaiser, J. W., Klimont, Z., Lohmann, U., Schwarz, J. P., Shindell, D., Storelvmo, T.,
850 Warren, S. G., and Zender, C. S.: Bounding the role of black carbon in the climate system: a scientific
851 assessment, *J. Geophys. Res. Atmos.*, 118, 5380-5552, 2013.
- 852
853 Bozzetti, C., Daellenbach, K. R., Hueglin, C., Fermo, P., Sciare, J., Kasper-Giebl, A., Mazar, Y.,
854 Abbaszade, G., El Kazzi, M., Gonzalez, R., Shuster-Meiseles, T., Flasch, M., Wolf, R., Křepelová, A.,



- 855 Canonaco, F., Schnelle-Kreis, J., Slowik, J. G., Zimmermann, R., Rudich, Y., Baltensperger, U., El
856 Haddad, I., and Prévôt, A. S. H.: Size-resolved identification, characterization, and quantification of
857 primary biological organic aerosol at a European rural site, *Environ. Sci. Technol.*, 50, 3425–3434,
858 2016.
- 859
- 860 Buchholz, B. A., Fallon, S. J., Zermeno, P., Bench, G., and Schichtel, B. A.: Anomalous elevated
861 radiocarbon measurements of PM_{2.5}, *Nucl. Instrum. Methods Phys. Res. B*, 294, 631–635,
862 doi:10.1016/j.nimb.2012.05.021, 2013.
- 863
- 864 Cassee, Flemming R., Heroux, M.-E., Gerlofs-Nijland, M. E., and Kelly, F. J.: Particulate matter
865 beyond mass: recent health evidence on the role of fractions, chemical constituents and sources of
866 emission, *Inhal Toxicol.*, 14, 802-12, doi:10.3109/08958378.2013.850127, 2013.
- 867
- 868 Ceburnis, D., Garbaras, A., Szidat, S., Rinaldi, M., Fahrni, S., Perron, N., Wacker, L., Leinert, S.,
869 Remeikis, V., Facchini, M. C., Prevot, A. S. H., Jennings, S. G., Ramonet, M., and O'Dowd, C. D.:
870 Quantification of the carbonaceous matter origin in submicron marine aerosol by ¹³C and ¹⁴C isotope
871 analysis, *Atmos. Chem. Phys.*, 11, 8593-8606, doi:10.5194/acp-11-8593-2011, 2011.
- 872
- 873 Ciarelli, G., El Haddad, I., Bruns, E., Aksoyoglu, S., Möhler, O., Baltensperger, U., and Prévôt, A. S.
874 H.: Constraining a hybrid volatility basis-set model for aging of wood-burning emissions using smog
875 chamber experiments: a box-model study based on the VBS scheme of the CAMx model (v5.40),
876 *Geosci. Model Dev.*, 10, 2303-2320, 2017.
- 877
- 878 Crippa, M., Canonaco, F., Lanz, V. A., Äijälä, M., Allan, J. D., Carbone, S., Capes, G., Ceburnis, D.,
879 Dall'Osto, M., Day, D. A., DeCarlo, P. F., Ehn, M., Eriksson, A., Freney, E., Hildebrandt Ruiz, L.,
880 Hillamo, R., Jimenez, J. L., Junninen, H., Kiendler-Scharr, A., Kortelainen, A.-M., Kulmala, M.,
881 Laaksonen, A., Mensah, A. A., Mohr, C., Nemitz, E., O'Dowd, C., Ovadnevaite, J., Pandis, S. N.,
882 Petäjä, T., Poulain, L., Saarikoski, S., Sellegrì, K., Swietlicki, E., Tiitta, P., Worsnop, D. R.,
883 Baltensperger, U., and Prévôt, A. S. H.: Organic aerosol components derived from 25 AMS data sets
884 across Europe using a consistent ME-2 based source apportionment approach, *Atmos. Chem. Phys.*, 14,
885 6159–6176, <https://doi.org/10.5194/acp-14-6159-2014>, 2014.
- 886
- 887 Crutzen, P. J. and Andreae, M. O.: Biomass burning in the tropics: impact on atmospheric chemistry
888 and biogeochemical cycles, *Science*, 250, 1669-1678, 1990.
- 889
- 890 Denier van der Gon, H. A. C., Bergström, R., Fountoukis, C., Johansson, C., Pandis, S. N., Simpson,
891 D., and Visschedijk, A. J. H.: Particulate emissions from residential wood combustion in Europe –
892 revised estimates and an evaluation, *Atmos. Chem. Phys.*, 15, 6503-6519, doi:10.5194/acp-15-6503-
893 2015, 2015a.
- 894



- 895 Denier van der Gon, H. A. C., Kuenen, J. J. P., and Visschedijk, A. J. H.: Personal communication,
896 2015b.
897
- 898 Diapouli, E., Popovicheva, O., Kistler, M., Vratolis, S., Persiantseva, N., Timofeev M., Kasper-Giebl,
899 A., and Eleftheriadis, K.: Physicochemical characterization of aged biomass burning aerosol after long-
900 range transport to Greece from large scale wildfires in Russia and surrounding regions, Summer 2010,
901 Atmos. Environ., 96, 393-404, 2014.
902
- 903 Dore, A. J., Carslaw, D. C., Braban, C., Cain, M., Chemel, C., Conolly, C., Derwent, R. G., Griffiths,
904 S. J., Hall, J., Hayman, G., Lawrence, S., Metcalfe, S. E., Redington, A., Simpson, D., Sutton, M. A.,
905 Sutton, P., Tang, Y. S., Vieno, M., Werner, M., Whyatt, J. D.: Evaluation of the performance of
906 different atmospheric chemical transport models and inter-comparison of nitrogen and sulphur
907 deposition estimates for the UK, Atmos. Environ., 119, 131-143, 2015.
908
- 909 Dye, C. and Yttri, K. E.: Determination of monosaccharide anhydrides in atmospheric aerosols by use
910 of high-resolution mass spectrometry combined with high performance liquid chromatography, Anal.
911 Chem., 77, 1853-1858, 2005.
912
- 913 Elsasser, M., Crippa, M., Orasche, J., DeCarlo, P. F., Oster, M., Pitz, M., Cyrus, J., Gustafson, T. L.,
914 Pettersson, J. B. C., Schnelle-Kreis, J., Prevot, A. S. H., and Zimmermann, R.: Organic molecular
915 markers and signature from wood combustion particles in winter ambient aerosols: aerosol mass
916 spectrometer (AMS) and high time-resolved GC-MS measurements in Augsburg, Germany, Atmos.
917 Chem. Physics, 12, 6113-6128, 2012.
918
- 919 Fahrni, S. M., Gäggeler, H. W., Hajdas, I., Ruff, M., Szidat, S., and Wacker, L.: Direct measurements
920 of small ^{14}C samples after oxidation in quartz tubes, Nucl. Instrum. Meth. Phys. Res. B., 268, 787-789,
921 doi:10.1016/j.nimb.2009.10.031, 2010.
922
- 923 Fuller, G. W., Tremper, A. H., Baker, T. D., Yttri, K. E., and Butterfield, D.: Contribution of wood
924 burning to PM₁₀ in London, Atmos. Environ., 87, 87-94. doi:10.1016/j.atmosenv.2013.12.037, 2014.
925
- 926 Gelencsér, A.: Carbonaceous Aerosol, Atmospheric and Oceanographic Science Library Series, vol.
927 30, Springer, New York, 2004.
928
- 929 Gelencsér, A., May, B., Simpson, D., Sánchez-Ochoa, A., Kasper-Giebl, A., Puxbaum, H., Caseiro, A.,
930 Pio, C., and Legrand, M.: Source apportionment of PM_{2.5} organic aerosol over Europe:
931 primary/secondary, natural/anthropogenic, fossil/biogenic origin, J. Geophys. Res., 112, D23S04, doi:
932 10.1029/2006JD008094, 2007.
933



- 934 Genberg, J., Hyder, M., Stenström, K., Bergström, R., Simpson, D., Fors, E. O., Jönsson, J. Å., and
935 Swietlicki, E.: Source apportionment of carbonaceous aerosol in southern Sweden, *Atmos. Chem.*
936 *Phys.*, 11, 11387–11400, <https://doi.org/10.5194/acp-11-11387-2011>, 2011.
937
- 938 Genberg, J., Denier van der Gon, H. A. C., Simpson, D., Swietlicki, E., Areskou, H., Beddows, D.,
939 Ceburnis, D., Fiebig, M., Hansson, H. C., Harrison, R. M., Jennings, S. G., Saarikoski, S., Spindler, G.,
940 Visschedijk, A. J. H., Wiedensohler, A., Yttri, K. E., and Bergström, R.: Light-absorbing carbon in
941 Europe – measurement and modelling, with a focus on residential wood combustion emissions, *Atmos.*
942 *Chem. Phys.*, 13, 8719–8738, doi:10.5194/acp-13-8719-2013, 2013.
943
- 944 Gianini, M. F. D., Fischer, A., Gehrig, R., Ulrich, A., Wichser, A., Piot, C., Besombes, J.-L., and
945 Hueglin, C.: Sources of PM₁₀ in Switzerland: an analysis for 2008/2009 and changes since 1998/1999,
946 *Atmos. Environ.*, 54, 149–158, 2012.
947
- 948 Gilardoni, S., Vignati, E., Cavalli, F., Putaud, J. P., Larsen, B. R., Karl, M., Stenström, K., Genberg, J.,
949 Henne, S., and Dentener, F.: Better constraints on sources of carbonaceous aerosols using a combined
950 14C - macro tracer analysis in a European rural background site, *Atmos. Chem. Physics*, 11, 5685–
951 5700, doi:10.5194/acp-11-5685-2011, 2011.
952
- 953 Glasius, M., Hansen, A. M. K., Claeys, M., Henzing, J. S., Jedynska, A. D., Kasper-Giebl, A., Kistler,
954 M., Kristensen, K., Martinsson, J., Maenhaut, W., Nøjgaard, J. K., Spindler, G., Stenström, K. E.,
955 Swietlicki, E., Szidat, S., Simpson, D., and Yttri, K. E.: Composition and sources of carbonaceous
956 aerosols in Northern Europe during winter, *Atmos. Environ.*, 173, 127–141,
957 doi:10.1016/j.atmosenv.2017.11.005, 2018.
958
- 959 Grieshop, A. P., Logue, J. M., Donahue, N. M., and Robinson, A. L.: Laboratory investigation of
960 photochemical oxidation of organic aerosol from wood fires 1: measurement and simulation of organic
961 aerosol evolution, *Atmos. Chem. Physics*, 9, 1263–1277, 2009.
962
- 963 Hallquist, M., Wenger, J. C., Baltensperger, U., Rudich, Y., Simpson, D., Claeys, M., Dommen, J.,
964 Donahue, N. M., George, C., Goldstein, A. H., Hamilton, J. F., Herrmann, H., Hoffmann, T., Iinuma,
965 Y., Jang, M., Jenkin, M. E., Jimenez, J. L., Kiendler-Scharr, A., Maenhaut, W., McFiggans, G., Mentel,
966 T. F., Monod, A., Prevot, A. S. H., Seinfeld, J. H., Surratt, J. D., Szmigielski, R., and Wildt, J.: The
967 formation, properties and impact of secondary organic aerosol: current and emerging issues,
968 *Atmospheric Chemistry and Physics*, 9, 5155–5236, [10.5194/acp-9-5155-2009](https://doi.org/10.5194/acp-9-5155-2009), 2009.
969
- 970 Hao, W.M., Petkov, A., Nordgren, B.R., Corley, R.E., Silverstein, R.P., Urbanski, S.P., Evangeliou, N.,
971 Balkanski, Y., and Kinder, B.L. Daily black carbon emissions from fires in northern Eurasia for 2002–
972 2015. *Geosci. Model Dev.*, 9, 4461–4474. www.geosci-model-dev.net/9/4461/2016/doi:10.5194/gmd-
973 9-4461-2016, 2016.



- 974
- 975 Heal, M. R., Naysmith, P., Cook, G. T., Xu, S., Duran, T. R., and Harrison, R. M.: Application of 14C
976 analyses to source apportionment of carbonaceous PM_{2.5} in the UK, *Atmos. Environ.*, 45, 2341-2348,
977 2011.
- 978
- 979 Henne, S., Brunner, D., Folini, D., Solberg, S., Klausen, J., and Buchmann, B.: Assessment of
980 parameters describing representativeness of air quality in-situ measurement sites, *Atmos. Chem. Phys.*,
981 10, 3561–3581, doi:10.5194/acp-10-3561-2010, 2010.
- 982
- 983 Herich, H., Gianini, M. F. D., Piot, C., Mocnik, G., Jaffrezo, J.-L., Besombes, J.-L., Prévôt, A. S. H.,
984 and Hueglin, C.: Overview of the impact of wood burning emissions on carbonaceous aerosols and PM
985 in large parts of the Alpine region, *Atmos. Environ.*, 89, 64-75, 2014.
- 986
- 987 Jathar, S. H., Gordon, T. D., Hennigan, C. J., Pye, H. O. T., Pouliot, G., Adams, P. J., Donahue, N. M.,
988 and Robinson, A. L.: Unspeciated organic emissions from combustion sources and their influence on
989 the secondary organic aerosol budget in the United States, *Proc. Natl. Acad. Sci. Unit. States Am*, 111,
990 10473-10478, 2014.
- 991
- 992 Kanakidou, M., Seinfeld, J. H., Pandis, S. N., Barnes, I., Dentener, F. J., Facchini, M. C., Van
993 Dingenen, R., Ervens, B., Nenes, A., Nielsen, C. J., Swietlicki, E., Putaud, J. P., Balkanski, Y., Fuzzi,
994 S., Horth, J., Moortgat, G. K., Winterhalter, R., Myhre, C. E. L., Tsigaridis, K., Vignati, E., Stephanou,
995 E. G., and Wilson, J.: Organic aerosol and global climate modelling: a review, *Atmos. Chem. Phys.*, 5,
996 1053–1123, doi:10.5194/acp-5-1053-2005, 2005.
- 997
- 998 Korontzi, S., McCarty, J., Loboda, T., Kumar, S., and Justice, C.: Global distribution of agricultural
999 fires in croplands from 3 years of Moderate Resolution Imaging Spectroradiometer (MODIS) data,
1000 *Global Biogeochem. Cycles*, 20, GB2021, doi:10.1029/2005GB002529, 2006.
- 1001
- 1002 Kourtchev, I., Copolovici, L., Claeys, M., and Maenhaut, W.: Characterization of atmospheric aerosols
1003 at a forested site in central Europe, *Environ. Sci. Technol.*, 43, 4665–4671, 2009.
- 1004
- 1005 Kristiansen, N. I., Stohl, A., and Wotawa, G.: Atmospheric removal times of the aerosol-bound
1006 radionuclides ¹³⁷Cs and ¹³¹I measured after the Fukushima Dai-ichi nuclear accident – a constraint for
1007 air quality and climate models, *Atmos. Chem. Phys.*, 12, 10759–10769, 2012.
- 1008
- 1009 Kuenen, J. J. P., Visschedijk, A. J. H., Jozwicka, M., and Denier van der Gon, H. A. C.: TNO-
1010 MACC_{II} emission inventory; a multi-year (2003–2009) consistent high-resolution European emission
1011 inventory for air quality modelling, *Atmos. Chem. Phys.*, 14, 10963-10976, doi:10.5194/acp-14-10963-
1012 2014, 2014.
- 1013



- 1014 Kulmala, M., Asmi, A., Lappalainen, H. K., Carslaw, K. S., Pöschl, U., Baltensperger, U., Hov, Ø.,
1015 Brenquier, J.-L., Pandis, S. N., Facchini, M. C., Hansson, H.-C., Wiedensohler, A., and O'Dowd, C.
1016 D.: Introduction: European Integrated Project on Aerosol Cloud Climate and Air Quality interactions
1017 (EUCAARI) – integrating aerosol research from nano to global scales, *Atmos. Chem. Phys.*, 9, 2825–
1018 2841, doi:10.5194/acp-9-2825-2009, 2009.
- 1019
1020 Liu, J., Li, J., Vonwiller, M., Liu, D., Cheng, H., Shen, K., Salazar, G., Agrios, K., Zhang, Y., Hea, Q.,
1021 Ding, X., Zhong, G., Wang, X., Szidat, S., and Zhang, G.: The importance of non-fossil sources in
1022 carbonaceous aerosols in a megacity of central China during the 2013 winter haze episode: A source
1023 apportionment constrained by radiocarbon and organic tracers, *Atmos. Environ.*, 144, 60–68,
1024 doi:10.1016/j.atmosenv.2016.08.068, 2016.
- 1025
1026 May, B., Wagenbach, D., Hammer, S., Steier, P., Puxbaum, H., and Pio, C.: The anthropogenic
1027 influence on carbonaceous aerosol in the European background, *Tellus B*, 61, 464–472, 2009.
- 1028
1029 May, A. A., Levin, E. J. T., Hennigan, C. J., Riipinen, I., Lee, T., Collett Jr., J. L., Jimenez, J. L.,
1030 Kreidenweis, S. M., and Robinson, A. L.: Gas-particle partitioning of primary organic aerosol
1031 emissions: 3. Biomass burning, *J. Geophys. Res. Atmos.*, 118, 11,327–11,338, doi:10.1002/jgrd.50828,
1032 2013a.
- 1033
1034 May, A. A., Presto, A. A., Hennigan, C. J., Nguyenm N. T., Gordon, T. D., and Robinson, A. L.: Gas-
1035 Particle Partitioning of Primary Organic Aerosol Emissions: (2) Diesel Vehicles, *Environ. Sci.*
1036 *Technol.*, 47, 8288–8296, doi:10.1021/es400782j, 2013b.
- 1037
1038 McDow, S. R. and Huntzicker, J. J.: Vapor adsorption artifact in the sampling of organic aerosol: face
1039 velocity effects, *Atmos. Environ.*, 24, 2563–2571, 1990.
- 1040
1041 Mohn, J., Szidat, S., Fellner, J., Rechberger, H., Quartier, R., Buchmann, B., and Emmenegger, L.:
1042 Determination of biogenic and fossil CO₂ emitted by waste incineration based on ¹⁴CO₂ and mass
1043 balances, *Bioresour. Technol.*, 99, 6471–6479, doi:10.1016/j.biortech.2007.11.042, 2008.
- 1044
1045 Novakov, T. and Penner, J.: Large contribution of organic aerosols to cloud condensation nuclei
1046 concentrations, *Nature*, 365, 823–826, 1993.
- 1047
1048 Ots, R., Young, D. E., Vieno, M., Xu, L., Dunmore, R. E., Allan, J. D., Coe, H., Williams, L. R.,
1049 Herndon, S. C., Ng, N. L., Hamilton, J. F., Bergström, R., Di Marco, C., Nemitz, E., Mackenzie, I. A.,
1050 Kuenen, J. J. P., Green, D. C., Reis, S., and Heal, M. R.: Simulating secondary organic aerosol from
1051 missing diesel-related intermediate-volatility organic compound emissions during the Clean Air for
1052 London (ClearfLo) campaign, *Atmos. Chem. Phys.*, 16, 6453–6473, [https://doi.org/10.5194/acp-16-](https://doi.org/10.5194/acp-16-6453-2016)
1053 6453-2016, 2016.



- 1054
- 1055 Pope, C. A. and Dockery, D. W.: Health effects of fine particulate air pollution: lines that connect., J.
1056 Air Waste Manag. Assoc., 56, 709-742, 2006.
- 1057
- 1058 Pöschl, U.: Aerosol particle analysis: challenges and progress, Anal. Bioanal. Chem., 375, 30–32,
1059 2003.
- 1060
- 1061 Pöschl, U.: Atmospheric aerosols: Composition, transformation, climate and health effects, Angew.
1062 Chem. Int. Ed., 44, 7520–7540. 2005.
- 1063
- 1064 Putaud, J.-P., R. Van Dingenen, A. Alastuey, H. Bauer, W. Birmili, J. Cyrys, H. Flentje, S. Fuzzi, R.
1065 Gehrig, H.C. Hansson, R.M. Harrison, H. Hermann, R. Hitzenberger, C. Hüglin, A.M. Jones, A.
1066 Kasper-Giebl, G. Kiss, A. Koussa, T.A.J. Kuhlbusch, G. Löschau, W. Maenhaut, A. Molnar, T. Moreno,
1067 J. Pekkanen, C. Perrino, M. Pitz, H. Puxbaum, X. Querol, S. Rodriguez, I. Salma, J. Schwarz, J.
1068 Smolik, J. Schneider, G. Spindler, H. ten Brink, J. Tursic, M. Viana, A. Wiedensohler, and F. Raes, A
1069 European Aerosol Phenomenology - 3: physical and chemical characteristics of particulate matter from
1070 60 rural, urban, and kerbside sites across Europe, Atmos. Environ. 44, 1308-1320, 2010.
- 1071
- 1072 Puxbaum, H., Caseiro, A., Sánchez-Ochoa, A., Kasper-Giebl, A., Claeys, M., Gelencsér, A., Legrand,
1073 M., Preunkert, S., Pio, C. A.: Levoglucosan levels at background sites in Europe for assessing the
1074 impact of biomass combustion on the European, aerosol background, J. Geophys. Res., 112, D23S05,
1075 doi:10.1029/2006JD008114, 2007.
- 1076
- 1077 Querol, X., Alastuey, A., Pey, J., Cusack, M., Pérez, N., Mihalopoulos, N., Theodosi, C.,
1078 Gerasopoulos, E., Kubilay, N., and Kocak, M.: Variability in regional background aerosols within the
1079 Mediterranean, Atmos. Chem. Phys., 9, 4575–4591, doi:10.5194/acp-9-4575-2009, 2009.
- 1080
- 1081 Reimer, P. J., Brown, T. A., and Reimer, R. W.: Discussion: Reporting and Calibration of PostBomb
1082 ¹⁴C Data, Radiocarbon, 46, 1299-1304, 2004.
- 1083
- 1084 Robinson, A. L., Donahue, N. M., Shrivastava, M. K., Weitkamp, E. A., Sage, A. M., Grieshop, A. P.,
1085 Lane, T. E., Pierce, J. R., and Pandis, S. N.: Rethinking Organic Aerosols: Semivolatile Emissions and
1086 Photochemical Aging, Science, 315, 1259-1262, 2007.
- 1087
- 1088 Rohr, A. C. and Wyzga, R. E.: Attributing health effects to individual particulate matter constituents,
1089 Atmos. Environ., 62, 130–152, doi:10.1016/j.atmosenv.2012.07.036, 2012.
- 1090
- 1091 Ruff, M., Wacker, L., Gäggeler, H. W., Suter, M., Synal, H. A., and Szidat, S.: A gas ion source for
1092 radiocarbon measurements at 200 kV, Radiocarbon, 49, 307-314, 2007.
- 1093



- 1094 Simpson, D., Yttri, K. E., Klimont, Z., Kupiainen, K., Caseiro, A., Gelencsér, A., Pio, C., Legrand, M.:
1095 Modeling carbonaceous aerosol over Europe. Analysis of the CARBOSOL and EMEP EC/OC
1096 campaigns, *J. Geophys. Res.*, 112, D23S14, doi:10.1029/2006JD008114, 2007.
1097
- 1098 Simpson, D., Benedictow, A., Berge, H., Bergström, R., Emberson, L. D., Fagerli, H., Flechard, C. R.,
1099 Hayman, G. D., Gauss, M., Jonson, J. E., Jenkin, M. E., Nyíri, A., Richter, C., Semeena, V. S., Tsyro,
1100 S., Tuovinen, J.-P., Valdebenito, Á., and Wind, P.: The EMEP MSC-W chemical transport model –
1101 technical description, *Atmos. Chem. Phys.*, 12, 7825–7865, doi:10.5194/acp-12-7825-2012, 2012.
1102
- 1103 Simpson, D. and Denier van der Gon, H.: Problematic emissions - particles or gases? in:
1104 Transboundary particulate matter, photo-oxidants, acidifying and eutrophying components, EMEP
1105 Status Report 1/2015, The Norwegian Meteorological Institute, Oslo, Norway, 87-96, 2015.
1106
- 1107 Simpson, D., Bergström, R., Imhof, H., and Wind, P.: Updates to the EMEP/MS-CW model, 2016-
1108 2017, in: Transboundary particulate matter, photo-oxidants, acidifying and eutrophying components,
1109 Status Report 1/2017, The Norwegian Meteorological Institute, Oslo, Norway, 115-122, 2017.
1110
- 1111 Spindler, G., Gnauk, T., Grüner, A., Iinuma, Y., Müller, K., Scheinhardt, S. and Herrmann, H.: Size-
1112 segregated characterization of PM₁₀ at the EMEPsite Melpitz (Germany) using a five-stage impactor: a
1113 six year study. *J. Atmos. Chem.*, 69, 127-157, 2012.
1114
- 1115 Stohl, A., Berg, T., Burkhart, J. F., Fjæraa, A. M., Forster, C., Herber, A., Hov, Ø., Lunder, C.,
1116 McMillan, W. W., Oltmans, S., Shiobara, M., Simpson, D., Solberg, S., Stebel, K., Ström, J., Tørseth,
1117 K., Treffeisen, R., Virkkunen, K., and Yttri, K. E.: Arctic smoke - record high air pollution levels in the
1118 European Arctic due to agricultural fires in Eastern Europe, *Atmos. Chem. Phys.*, 7, 511–534, 2007.
1119
- 1120 Subramanian, R., Khlystov, A. Y., and Robinson, A. L.: Effect of Peak Inert-Mode Temperature on
1121 Elemental Carbon Measured Using Thermal-Optical Analysis, *Aerosol Science and Technology*, 40:10,
1122 763–780, doi: 10.1080/02786820600714403, 2006.
1123
- 1124 Szidat, S., Jenk, T. M., Gäggeler, H. W., Synal, H. A., Fisseha, R., Baltensperger, U., Kalberer, M.,
1125 Samburova, V., Reimann, S., Kasper-Giebl, A., and Hajdas, I.: Radiocarbon (¹⁴C)-deduced biogenic
1126 and anthropogenic contributions to organic carbon (OC) of urban aerosols from Zurich, Switzerland,
1127 *Atmos. Environ.*, 38, 4035–4044, 2004.
1128
- 1129 Szidat, S., Prevot, A. S. H., Sandradewi, J., Alfarra, M. R., Synal, H.-A., Wacker, L., Baltensperger, U.:
1130 Dominant impact of residential wood burning on particulate matter in Alpine valleys during winter,
1131 *Geophys. Res. Lett.*, 34, L05820, doi:10.1029/2006GL028325, 2007.
1132



- 1133 Szidat, S., Ruff, M., Perron, N., Wacker, L., Synal, H.-A., Hallquist, M., Shannigrahi, A. S., Yttri, K.
1134 E., Dye, C., and Simpson, D.: Fossil and non-fossil sources of organic carbon (OC) and elemental
1135 carbon (EC) in Göteborg, Sweden. *Atmos. Chem. Phys.* 9, 1521–1535, doi:10.5194/acp-9-1521-2009,
1136 2009.
- 1137 Viana, M., Kuhlbusch, T. A., Querol, X., Alastuey, A., Harrison, R. M., Hopke, P. K., Winiwarter, W.,
1138 Vallius, M., Szidat, S., Prevot, A. S. H., Hueglin, C., Bloemen, H., Wahlin, P., Vecchi, R., Miranda, A.
1139 I., Kasper-Giebl, A., Maenhaut, W., Hitzenberger, R.: Source apportionment of particulate matter in
1140 Europe: a review of methods and results, *J. Aerosol Sci.*, 39, 827–849,
1141 doi:10.1016/j.jaerosci.2008.05.007, 2008.
- 1142
- 1143 Vieno, M., Heal, M. R., Williams, M. L., Carnell, E. J., Nemitz, E., Stedman, J. R., and Reis, S.: The
1144 sensitivities of emissions reductions for the mitigation of UK PM_{2.5}, *Atmos. Chem. Phys.*, 16, 265–276,
1145 <https://doi.org/10.5194/acp-16-265-2016>, 2016.
- 1146
- 1147 Wacker, L., Fahrni, S. M., Hajdas, I., Molnar, M., Synal, H.-A., Szidat, S., and Zhang, Y.L.: A versatile
1148 gas interface for routine radiocarbon analysis with a gas ion source, *Nucl. Instr. Meth. Phys. Res. B*,
1149 294, 315–319, doi:10.1016/j.nimb.2012.02.009, 2013.
- 1150
- 1151 Wagener, S., Langner, M., Hansen, U., Moriske, H. J., Endlicher, W. R., and Wilfried, R.: Spatial and
1152 seasonal variations of biogenic tracer compounds in ambient PM₁₀ and PM₁ samples in Berlin,
1153 Germany, *Atmos. Environ.*, 47, 33–42, doi:10.1016/j.atmosenv.2011.11.044, 2012.
- 1154
- 1155 Waked, A., Favez, O., Alleman, L. Y., Piot, C., Petit, J.-E., Delaunay, T., Verlinden, E., Golly, B.,
1156 Besombes, J.-L., Jaffrezo, J.-L., and Leoz-Garziandia, E.: Source apportionment of PM₁₀ in a north-
1157 western Europe regional urban background site (Lens, France) using positive matrix factorization and
1158 including primary biogenic emissions, *Atmos. Chem. Phys.*, 14, 3325–3346,
1159 <https://doi.org/10.5194/acp-14-3325-2014>, 2014.
- 1160
- 1161 Wallén, A., Lidén, G., and Hansson H. C.: Measured Elemental Carbon by Thermo-Optical
1162 Transmittance Analysis in Water-Soluble Extracts from Diesel Exhaust, Woodsmoke, and Ambient
1163 Particulate Samples, *J. Occup. Environ. Med.*, 7, 35–41, doi: 10.1080/15459620903368859, 2010.
- 1164
- 1165 Wiedinmyer, C., Yokelson, R. J., and Gullett, B. K.: Global Emissions of Trace Gases, Particulate
1166 Matter, and Hazardous Air Pollutants from Open Burning of Domestic Waste, *Environ. Sci. Technol.*,
1167 48, 9523–9530, 2014.
- 1168
- 1169 Winiwarter, W., Bauer, H., Caseiro, A., and Puxbaum, H.: Quantifying emissions of primary biological
1170 aerosol particle mass in Europe, *Atmos. Environ.*, 43, 1403–1409, 2009.
- 1171



- 1172 Yang, H. and Yu, J. Z.: Uncertainties in Charring Correction in the Analysis of Elemental and Organic
1173 Carbon in Atmospheric Particles by Thermal/Optical Methods, *Environ Sci Technol.*, 36,5199-5204,
1174 2002.
1175
- 1176 Yttri, K. E., Aas, W., Bjerke, A., Cape, J. N., Cavalli, F., Ceburnis, D., Dye, C., Emblico, L., Facchini,
1177 M. C., Forster, C., Hanssen, J. E., Hansson, H. C., Jennings, S. G., Maenhaut, W., Putaud, J. P.,
1178 Tørseth, K.: Elemental and organic carbon in PM₁₀: A one year measurement campaign within the
1179 European monitoring and Evaluation Programme EMEP, *Atmos. Chem. Phys.*, 7, 5711-5725, 2007a.
1180
- 1181 Yttri, K. E., Dye, C., Kiss, G.: Ambient aerosol concentrations of sugars and sugar-alcohols at four
1182 different sites in Norway, *Atmos. Chem. Phys.*, 7, 4267-4279, 2007b.
1183
- 1184 Yttri, K. E., Simpson, D., Stenström, K., Puxbaum, H., and Svendby, T.: Source apportionment of the
1185 carbonaceous aerosol in Norway quantitative estimates based on ¹⁴C, thermal-optical and organic tracer
1186 analysis, *Atmos. Chem. Phys.*, 11, 9375–9394, doi:10.5194/acp-11-9375-2011, 2011a.
1187
- 1188 Yttri, K. E., Simpson, D., Nøjgaard, J. K., Kristensen, K., Genberg, J., Stenström, K., Swietlicki, E.,
1189 Hillamo, R., Aurela, M., Bauer, H., Offenberg, J. H., Jaoui, M., Dye, C., Eckhardt, S., Burkhart, J. F.,
1190 Stohl, A., and Glasius, M.: Source apportionment of the summer time carbonaceous aerosol at Nordic
1191 rural background sites, *Atmos. Chem. Phys.*, 11, 13339–13357, doi:10.5194/acp- 11-13339-2011,
1192 2011b.
1193
- 1194 Yttri, K. E., Lund Myhre, C., Eckhardt, S., Fiebig, M., Dye, C., Hirdman, D., Ström, J., Klimont, Z.,
1195 Stohl, A. (2014) Quantifying black carbon from biomass burning by means of levoglucosan – a one-
1196 year time series at the Arctic observatory Zeppelin. *Atmos. Chem. Phys.*, 14, 6427-6442,
1197 doi:10.5194/acp-14-6427-2014, 2014.
1198
- 1199 Yttri, K. E., Schnelle-Kreis, J., Maenhaut, W., Abbaszade, G., Alves, C., Bjerke, A., Bonnier, N.,
1200 Bossi, R., Claeys, M., Dye, C., Evtyugina, M., García-Gacio, D., Hillamo, R., Hoffer, A., Hyder, M.,
1201 Iinuma, Y., Jaffrezo, J.-L., Kasper-Giebl, A., Kiss, G., López-Mahia, P. L., Pio, C., Piot, C., Ramirez-
1202 Santa-Cruz, C., Sciare, J., Teinilä, K., Vermeylen, R., Vicente, A., Zimmermann, R. (2015) An
1203 intercomparison study of analytical methods used for quantification of levoglucosan in ambient aerosol
1204 filter samples, *Atmos. Meas. Tech.*, 8, 125-147, doi:10.5194/amt-8-125-2015, 2015.
1205
- 1206 Zappoli, S., Andracchio, A., Fuzzi, S., Facchini, M. C., Gelencsér, A., Kiss, G., Krivácsy, Z., Molnár,
1207 Á., Mészáros, E., Hansson, H. -C., Rosman, K., and Zebühr, Y.: Inorganic, organic and
1208 macromolecular components of fine aerosol in different areas of Europe in relation to their water
1209 solubility, *Atmos. Environ.*, 33, 2733–2743, [https://doi.org/10.1016/S1352-2310\(98\)00362-8](https://doi.org/10.1016/S1352-2310(98)00362-8), 1999.
1210



- 1211 Zhang, Q., Jimenez, J. L., Canagaratna, M. R., Allan, J. D., Coe, H., Ulbrich, I., Alfarra, M. R.,
1212 Takami, A., Middlebrook, A. M., Sun, Y. L., Dzepina, K., Dunlea, E., Docherty, K., DeCarlo, P. F.,
1213 Salcedo, D., Onasch, T., Jayne, J. T., Miyoshi, T., Shimono, A., Hatakeyama, Takegawa, N., Kondo,
1214 Y., Schneider, J., Drewnick, F., Borrmann, S., Weimer, S., Demerjian, K., Williams, P., Bower, K.,
1215 Bahreini, R., Cottrell, L., Griffin, R. J., Rautiainen, J., Sun, J. Y., Zhang, Y. M., and Worsnop, D. R.:
1216 Ubiquity and dominance of oxygenated species in organic aerosols in anthropogenically-influenced
1217 Northern Hemisphere midlatitudes, *Geophys. Res. Lett.*, 34, L13801, doi:10.1029/2007GL029979,
1218 2007.
- 1219
- 1220 Ziemann, PJ, Atkinson, R: Kinetics, products, and mechanisms of secondary organic aerosol formation,
1221 *Chem. Soc. Rev.*, 41, 6582-6605, doi:10.1039/c2cs35122f, 2012.
- 1222
- 1223 Zotter, P., Ciobanu, V. G., Zhang, Y. L., El-Haddad, I., Macchia, M., Daellenbach, K. R., Salazar, G.
1224 A., Huang, R.-J., Wacker, L., Hueglin, C., Piazzalunga, A., Fermo, P., Schwikowski, M.,
1225 Baltensperger, U., Szidat, S., and Prévôt, A. S. H.: Radiocarbon analysis of elemental and organic
1226 carbon in Switzerland during winter-smog episodes from 2008 to 2012 -- Part 1: Source apportionment
1227 and spatial variability, *Atmos. Chem. Phys.*, 14, 13551-13570, 2014.



Table 1: Location of the nine European rural background sites that participated in the Fall 2008 and Winter/spring 2009 sampling periods. The sites are ordered by latitude from south to north.

| Sampling site | Location | Height (m asl) | Sampling period | Cut-off size | Flow rate (l min ⁻¹) | Filter face velocity (cm s ⁻¹) | Ambient temp. (min-max) | Precip. (min-max) |
|-----------------------|---------------------|----------------|--------------------------------------|-------------------|----------------------------------|--|-----------------------------------|------------------------------------|
| Montelbretti (Italy) | 42° 06'N, 12° 38'E | 48 | 24.09–15.10.2008 25.02–25.03.2009 | PM ₁₀ | 38 | 54 | 16.8 (16.2–17.1) 9.9 (8.5–11) | 0.8 (0–2.4) 16.6 (1.2–45.8) |
| Ispra (Italy) | 45° 48'N, 08° 38'E | 209 | 24.09–22.10.2008 25.02–25.03.2009 | PM ₁₀ | 16.7 | 20 | 13.0 (12.8–13.3) 8.0 (7–9.6) | NA NA |
| Payerne (Switzerland) | 46° 48'N, 06° 56'E | 489 | 16.09–16.10.2008 27.02–25.03.2009 | PM ₁₀ | 16.7 | 23 | 10.5 (9.2–12.5) 4.4 (2.9–6.5) | 1.4 (0.6–2.5) 1.4 (0–3.9) |
| K-puszta (Hungary) | 46° 58'N, 19° 33'E | 130 | 17.09–15.10.2008 25.02–25.03.2009 | PM ₁₀ | 16.7 | 22 | 11.7 (9.9–12.6) 5.1 (3.7–7.2) | 9.3 (0–19.4) 5.3 (1.3–10.5) |
| Košetice (Czech Rep.) | 49° 35'N, 15° 05'E | 534 | 17.09–15.10.2008 25.02–25.03.2009 | PM ₁₀ | 38 | 53 | 9.6 (7.5–11.9) 2.0 (0.4–3.4) | 7.4 (2.7–16.6) 17.3 (11.3–23.2) |
| Melpitz (Germany) | 51° 32' N, 12° 54'E | 87 | 17.09–15.10.2008 25.02–25.03.2009 | PM ₁₀ | 16.7 | 22 | 11.2 (10.6–12.3) 5.4 (3.7–6.8) | 7.6 (3.1–14.3) 13.2 (9.5–16.6) |
| Mace Head (Ireland) | 53° 19'N, 09° 53'W | 15 | 18.09–15.10.2008 25.02–25.03.2009 | PM _{2.5} | 1111 | 45 | 12.4 (11.3–12.9) 8.3 (7.1–9.4) | 17.3 (0–51.2) 12.4 (0.1–37.1) |
| Lille Valby (Denmark) | 55° 41'N, 12° 08'E | 10 | 17.09–15.09.2008 25.02–25.03.2009 | PM ₁₀ | 38 | 56 | 10.9 (9.2–12) 5.2 (2.7–10.3) | 7.6 (0.3–21.7) 9.7 (3.321.3) |
| Birkenes (Norway) | 58° 23'N, 8° 15'E | 190 | 17.09–15.10.2008 25.02–25.03.2009 | PM ₁₀ | 38 | 54 | 8.2 (6–9.4) -0.7 (-1.5–0.3) | 31.1 (7.6–53.1) 22.5 (0.2–48.5) |



Table 2a: Mean (\pm SD) concentrations of carbonaceous sub-fractions and levoglucosan in PM_{10}^1 during Winter/Spring 2009. The EC/TC_p ratio, the OC_{Back}/OC_{Front} ratio and non-fossil fractions of TC_p ($f_{nt}(TC_p)$) are also listed. The sites are ordered by latitude from south to north.

| | Montelibretti | Ispra | Payerne | K-puszta | Košice | Melpitz | Mace Head ¹ | Lille Valby | Birkenes |
|--|-----------------|-----------------|-----------------|-----------------|-----------------|-----------------|------------------------|-----------------|-----------------|
| <i>Unit: ($\mu\text{g C m}^{-3}$)</i> | | | | | | | | | |
| TC _p | 6.1 \pm 2.7 | 9.3 \pm 5.7 | 3.6 \pm 1.3 | 5.5 \pm 2.8 | 2.1 \pm 0.78 | 1.7 \pm 0.68 | 0.76 \pm 0.91 | 1.5 \pm 0.33 | 0.44 \pm 0.13 |
| OC _p | 5.0 \pm 2.5 | 7.9 \pm 5.0 | 2.9 \pm 1.0 | 4.8 \pm 2.6 | 1.8 \pm 0.70 | 1.3 \pm 0.50 | 0.65 \pm 0.79 | 1.2 \pm 0.3 | 0.34 \pm 0.08 |
| OC _{Back} | 0.62 \pm 0.16 | 0.50 \pm 0.22 | 0.41 \pm 0.18 | 0.35 \pm 0.10 | 0.23 \pm 0.09 | 0.41 \pm 0.26 | 0.07 \pm 0.04 | 0.53 \pm 0.31 | 0.13 \pm 0.13 |
| EC | 1.0 \pm 0.25 | 1.5 \pm 0.68 | 0.66 \pm 0.27 | 0.77 \pm 0.21 | 0.32 \pm 0.12 | 0.40 \pm 0.12 | 0.11 \pm 0.13 | 0.37 \pm 0.09 | 0.10 \pm 0.05 |
| <i>Unit: (%)</i> | | | | | | | | | |
| EC/TC _p | 18 \pm 3.6 | 17 \pm 2.3 | 19 \pm 2.9 | 15 \pm 3.3 | 16 \pm 1.4 | 24 \pm 4.1 | 14 \pm 1.3 | 24 \pm 5.4 | 21 \pm 5.2 |
| OC _{Back} /OC _{Front} | 12 \pm 2.9 | 6.6 \pm 1.3 | 12 \pm 1.9 | 7.3 \pm 1.4 | 12 \pm 4.4 | 24 \pm 12 | 23 \pm 21 | 30 \pm 10 | 24 \pm 13 |
| <i>Unit: (Fraction)</i> | | | | | | | | | |
| $f_{nt}(TC_p)$ | 0.80 \pm 0.06 | 0.80 \pm 0.05 | 0.90 \pm 0.09 | 0.83 \pm 0.09 | 0.69 \pm 0.04 | 0.83 \pm 0.13 | 0.79 \pm 0.11 | 0.71 \pm 0.13 | 0.77 \pm 0.09 |
| <i>Unit: (ng m⁻³)</i> | | | | | | | | | |
| Levoglucosan | 247 \pm 113 | 668 \pm 295 | 141 \pm 63 | 209 \pm 156 | 67 \pm 16 | 57 \pm 20 | 12 \pm 13 | 41 \pm 5.5 | 17 \pm 7.7 |

¹) For Mace Head $PM_{2.5}$ was used



Table 2b: Mean (\pm SD) concentrations of carbonaceous sub-fractions and levoglucosan in PM_{10}^1 during Fall 2008. The EC/TC_p ratio, the OC_{Back}/OC_{Front} ratio and non-fossil fractions of TC_p ($f_{nt}(TC_p)$) are also listed. The sites are ordered from by latitude south to north.

| | Montelibretti ² | Ispra | Payerne | K-pusza | Košétece | Melpitz | Mace Head ¹ | Lille Valby | Birkenes |
|--|----------------------------|-----------------|-----------------|-----------------|-----------------|-----------------|------------------------|-----------------|-----------------|
| <i>Unit: ($\mu\text{g C m}^{-3}$)</i> | | | | | | | | | |
| TC _p | 5.0 \pm 1.8 | 7.6 \pm 2.5 | 3.9 \pm 1.1 | 6.7 \pm 2.9 | 3.3 \pm 0.66 | 2.1 \pm 0.36 | 0.89 \pm 1.2 | 1.8 \pm 0.74 | 1.1 \pm 0.47 |
| OC _p | 4.0 \pm 1.8 | 6.1 \pm 2.0 | 3.3 \pm 0.93 | 5.5 \pm 2.7 | 2.8 \pm 0.59 | 1.6 \pm 0.21 | 0.77 \pm 1.1 | 1.3 \pm 0.70 | 0.97 \pm 0.45 |
| OC _{Back} | 0.75 \pm 0.16 | 0.47 \pm 0.31 | 0.53 \pm 0.37 | 0.33 \pm 0.08 | 0.21 \pm 0.08 | 0.60 \pm 0.33 | 0.10 \pm 0.07 | 0.48 \pm 0.21 | 0.17 \pm 0.03 |
| EC | 0.97 \pm 0.25 | 1.5 \pm 0.54 | 0.59 \pm 0.17 | 1.2 \pm 0.26 | 0.49 \pm 0.10 | 0.54 \pm 0.16 | 0.12 \pm 0.17 | 0.46 \pm 0.10 | 0.11 \pm 0.03 |
| <i>Unit: (%)</i> | | | | | | | | | |
| EC/TC _p | 21 \pm 8.3 | 20 \pm 3.7 | 15 \pm 0.31 | 18 \pm 4.0 | 15 \pm 2.1 | 25 \pm 3.7 | 12 \pm 5.6 | 28 \pm 8.1 | 11 \pm 3.3 |
| OC _{Back} /OC _{Front} | 17 \pm 3.8 | 6.8 \pm 2.6 | 13 \pm 4.9 | 5.9 \pm 1.0 | 6.9 \pm 1.5 | 26 \pm 10 | 19 \pm 8.9 | 28 \pm 13 | 19 \pm 6.7 |
| <i>Unit: (Fraction)</i> | | | | | | | | | |
| $f_{nt}(TC_p)$ | 0.61 \pm 0.01 | 0.69 \pm 0.08 | 0.80 \pm 0.06 | 0.81 \pm 0.03 | 0.86 \pm 0.10 | 0.76 \pm 0.04 | 0.70 \pm 0.18 | 0.72 \pm 0.12 | 0.75 \pm 0.05 |
| <i>Unit: (ng m^{-3})</i> | | | | | | | | | |
| Levoglucosan | 106 \pm 40 | 364 \pm 180 | 85 \pm 16 | 172 \pm 84 | 83 \pm 14 | 33 \pm 14 | 16 \pm 19 | 32 \pm 19 | 6.8 \pm 2.2 |

1) For Mace Head $PM_{2.5}$ was used.

2) The sampler at Montelibretti was run in an alternating on/off mode, collecting ambient air 15 minutes every 1 hour.


Table 3: Volatility distributions of the primary organic aerosol (POA) emissions from anthropogenic sources.

| C^* ($\mu\text{g m}^{-3}$) ^a | | 10^{-2} | 10^{-1} | 1 | 10 | 10^2 | 10^3 | 10^4 | 10^5 | 10^6 |
|---|-------------------|-----------|-----------|-------|-------|--------|--------|--------|--------|--------|
| Base-case emission fraction^b | SNAP 2 | 0.20 | 0.00 | 0.10 | 0.10 | 0.20 | 0.40 | 0.00 | 0.00 | 0.00 |
| | all other sources | 0.00 | 0.04 | 0.25 | 0.37 | 0.23 | 0.11 | 0.00 | 0.00 | 0.00 |
| DT+IVOC emission fraction^{c, d} | SNAP 2 | 0.025 | 0.050 | 0.076 | 0.118 | 0.151 | 0.252 | 0.336 | 0.42 | 0.672 |
| | all other sources | 0.03 | 0.06 | 0.09 | 0.14 | 0.18 | 0.30 | 0.40 | 0.50 | 0.80 |

^a C^* : Saturation concentration at 298 K; enthalpies of vaporization were taken from May et al. (2013a,b) for the base-case (MACC-III), and from Shrivastava et al. (2008) for the DT+IVOC case.

^b The volatility distribution in the MACC-III model run is based on the recommended volatility distributions from May et al. (2013a,b) for biomass burning emissions (for SNAP sector 2; non-industrial stationary combustion) and for diesel exhaust (for all the other emission sectors), but moving the emissions in the $C^*=10^4 \mu\text{g m}^{-3}$ – $10^6 \mu\text{g m}^{-3}$ bins to the $10^3 \mu\text{g m}^{-3}$ bin.

^c The volatility distributions in the DT+IVOC case are based on Shrivastava et al. (2008) for all emission sectors except SNAP-2, for which it is based on the distribution used for the EMEP model in Denier van der Gon et al. (2015a). Note that this scenario assumes that there are substantial IVOC emissions that are not included in the emission inventories (see Bergström et al., 2012, and Denier van der Gon et al., 2015a).

^d Since the DT emission inventory by Denier van der Gon et al. (2015a) was constructed to include a larger fraction of SVOC from residential wood burning emissions, we apply a slightly different emission split for the SNAP-2 POA compared to other SNAP sectors. Considering both SVOC and IVOC within the POA class, the total POA emissions are assumed to be 2.1 times the inventory (compared to the factor 2.5 for the other emission sectors).



Table 4: Model and source apportioned (LHS-derived) concentrations of elemental carbon (EC_{bb}) and organic carbon (OC_{bb}) from biomass burning. Model results are averages over both measurement periods (Fall 2008 and Winter/Spring 2009). For the LHS-results the mean of the 10- and 90-percentiles are shown. Unit: $\mu\text{g C m}^{-3}$.

| Site | EC_{bb} | | | | OC_{bb} | | | |
|---------------|-----------|---------|--------|--------|-----------|---------|--------|--------|
| | Base-case | DT+IVOC | LHS-10 | LHS-90 | Base-case | DT+IVOC | LHS-10 | LHS-90 |
| Montelibretti | 0.19 | 0.097 | 0.29 | 0.70 | 0.28 | 0.37 | 1.04 | 2.38 |
| Ispra | 0.34 | 0.21 | 0.47 | 0.93 | 0.63 | 0.82 | 1.70 | 3.16 |
| K-pusztá | 0.20 | 0.17 | 0.30 | 0.67 | 0.37 | 0.74 | 1.10 | 2.27 |
| Payerne | 0.081 | 0.24 | 0.20 | 0.46 | 0.12 | 0.79 | 0.73 | 1.51 |
| Koščice | 0.074 | 0.17 | 0.12 | 0.28 | 0.14 | 0.60 | 0.42 | 0.91 |
| Melpitz | 0.063 | 0.096 | 0.085 | 0.18 | 0.12 | 0.37 | 0.30 | 0.57 |
| Mace Head | 0.0045 | 0.0091 | 0.028 | 0.057 | 0.015 | 0.061 | 0.086 | 0.16 |
| Lille Valby | 0.24 | 0.18 | 0.067 | 0.14 | 0.22 | 0.36 | 0.24 | 0.46 |
| Birkenes | 0.065 | 0.047 | 0.020 | 0.046 | 0.13 | 0.17 | 0.072 | 0.15 |



Figure 1: Overview of sampling sites participating in the carbonaceous aerosol source-apportionment study in the EMEP intensive measurement periods (IMPs) in Fall 2008 and Winter/spring 2009.

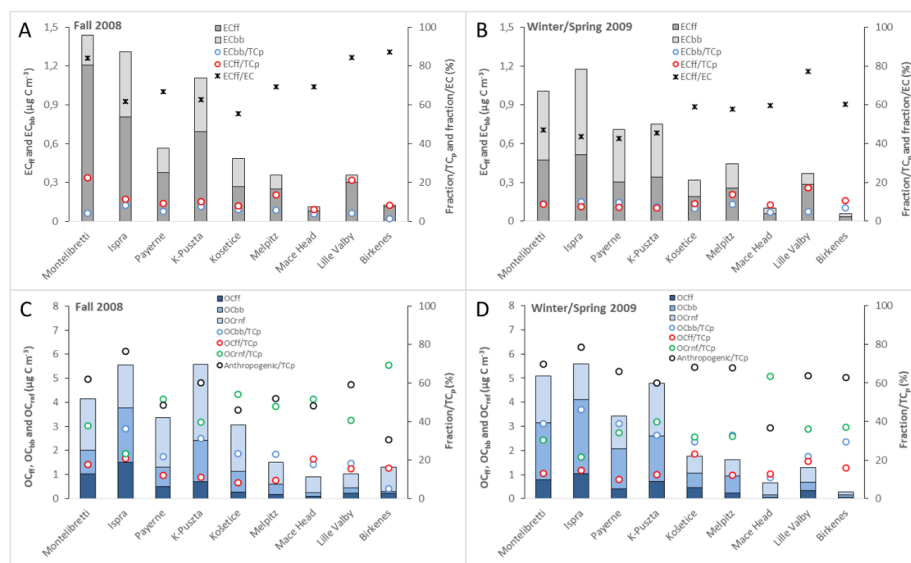


Figure 2: Mass concentrations of EC from fossil fuel (EC_{ff}) and biomass burning (EC_{bb}) sources, their fraction of particulate total carbon (TC_p) and the fraction of EC_{ff} to EC for Fall 2008 (panel A) and Winter/Spring 2009 (panel B). Mass concentrations of OC from fossil fuel (OC_{ff}), biomass burning (OC_{bb}) and remaining non-fossil (OC_{nrnf}) sources, their fraction of TC_p and the fraction of Anthropogenic (OC_{ff}, OC_{bb} EC_{ff} and EC_{bb}) to TC_p for Fall 2008 (panel C) and winter/spring 2009 (panel D). The sites are listed by latitude from South to North. Note that the EC_{ff}/TC_p marker is superimposed on the EC_{bb}/TC_p marker for Montelibretti and K-pusztá in panel B, and that the OC_{ff}/TC_p marker is superimposed on the OC_{bb}/TC_p marker for Montelibretti in panel C.

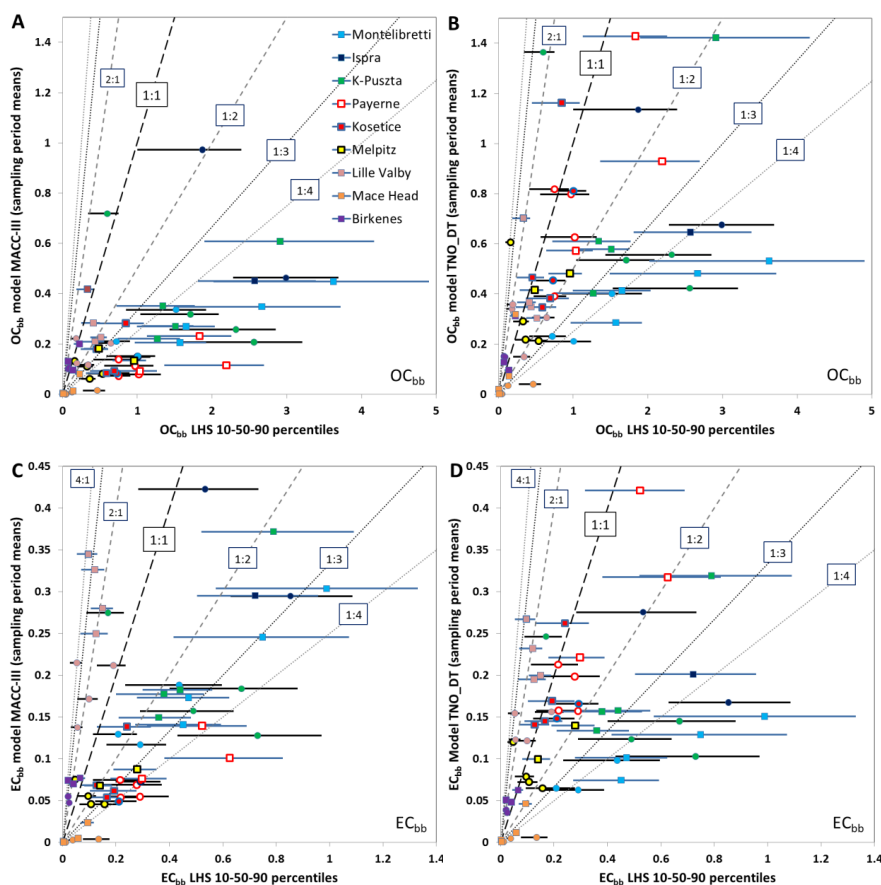


Figure 3: Comparison of modelled and measurement/LHS based concentrations of organic and elemental carbon from biomass burning emissions (OC_{bb} and EC_{bb}). The left panels (A and C) show model calculated OC_{bb} (A) and EC_{bb} (C) with the base-case model setup, and the right panels (B and D) show the corresponding results using the DT+IVOC model setup. Each point (and horizontal line) represents the results from a single site and week. The lines illustrate the range from the LHS 10-percentile to the 90-percentile and the circles and squares show the LHS-median values. Circles and black horizontal lines show results for Fall 2008 and squares and blue lines show results from Winter/spring 2009. The different sites are identified as follows: Light Blue – Montelibretti; Dark Blue – Ispra; Green – K-pusztza; White with red border – Payerne; Red with blue border – Košetice; Yellow with black border – Melpitz; Pink – Lille Valby; Orange – Mace Head; Purple – Birkenes. Unit: $\mu\text{g C m}^{-3}$.